Available online at www.sciencedirect.com
ScienceDirect
Geochimica et Cosmochimica Acta 71 (2007) 723–744
Geochimica
www.elsevier.com/locate/gca

Fluid inclusions in diamonds from the Diavik mine, Canada and the evolution of diamond-forming fluids

Ofra Klein-BenDavid [a,1], Elad S. Izraeli [b], Erik Hauri [c], Oded Navon [a,*]

[a] *Institute of Earth Sciences, The Hebrew University of Jerusalem, Jerusalem 91904, Israel*
[b] *Division of Identification and Forensics Science, Israel police headquarters, Jerusalem 91906, Israel*
[c] *Department of Terrestrial Magnetism, Carnegie Institution of Washington, 5241 Broad Branch Road, N.W., Washington, DC 20015, USA*

Received 9 February 2006; accepted in revised form 2 October 2006

Abstract

The analysis of micro-inclusions in fibrous diamonds from the Diavik mine, Canada revealed the presence of high density fluids (HDFs) that span a continuous compositional range between carbonatitic and saline end-members. The carbonatitic end-member is rich in Na, Ca, Mg, Fe, Ba and carbonate; the saline one is rich in K, Cl and water. In molar proportions, the composition of the saline end-member is: $K_{38}Na_{7.7}Ca_{1.8}Mg_{1.6}Fe_{1.5}Ba_{1.9}SiO_{3.1}Cl_{46}(CO_3)_{5.5}(H_2O)_{56}$ and that of the carbonatitic end member is: $K_{15}Na_{21}Ca_{6.7}Mg_{8.1}Fe_{6.2}Ba_{5.7}Si_{4.8}Ti_{1.4}Al_{1.9}O_{17}Cl_{29}(CO_3)_{29}(H_2O)_{29}$. The micro-inclusions in one diamond span a narrow range between a silicic end-member (rich in Si, K and water) and a carbonatitic one (rich in Mg, Ca, Fe and carbonate). Its average composition is: $K_{26}Na_{5.5}Ca_{13.8}Mg_{8.3}Fe_{9.6}Ba_{0.9}P_{2.5}Si_{25}Ti_{1.6}Al_{3.8}Cl_{2.5}O_{81}(CO_3)_{29}(H_2O)_{78}$. Thus, the Diavik diamonds span most of the known compositional range for fluids trapped in diamonds. Based on these data and previous analyses of fluids trapped in diamonds, we discuss possible models for the evolution of diamond-forming fluids. The most plausible model is where carbonatitic-HDFs are parental to all the other compositions. They evolve by fractionation of divalentions- and alkali-carbonates and by immiscible separation into saline- and silicic-HDFs. Each phase continues to evolve separately, crystallizing carbonates, diamond, and accessory silicates, phosphates, halides and more of the immiscible phase. Other processes, like the mixing of evolved fluids with fresh parental carbonatitic fluids, or metasomatic interactions with the wallrock also play a role in the evolution of the HDFs. We also propose that the parental carbonatitic-HDF evolves through fractional crystallization of an alkali-rich, low degree melt that is similar to the high pressure parental melts of kimberlites or lamproites.

1. Introduction

Diamond inclusions provide a unique opportunity to investigate the mantle rocks within which diamonds are formed as well as the fluids from which they crystallize. The diamond's strength and its low reactivity in a silicate environment ensure that trapped material within the diamond remains shielded from the changing environment. Mineral inclusions, ranging in size from less than a micrometer (Klein-BenDavid et al., 2006) to a fraction of a millimeter (Smith et al., 1991; Sobolev et al., 1999), are found in many diamonds. They consist of silicates, oxides, sulfides, and rare carbonates and provide information on host-rock lithology and on the temperatures and pressures at diamond crystallization (Meyer, 1987; Harris, 1992). Most mineral inclusions indicate growth in peridotitic or eclogitic environments, at temperatures of 900–1300 °C, and depths of 150–200 km (Meyer, 1987; Harris, 1992; Sobolev et al., 1997).

The symmetrical internal structure of diamonds (Milledge et al., 1984; Bulanova, 1995), the low density of crystallographic dislocations (Sunagawa, 1984), and the association of diamonds with cracks and secondary minerals within their host xenoliths (Taylor et al., 2000; Taylor and Anand, 2004) indicate that most of the natural diamonds grow from fluids. Fluid inclusions in diamonds are the best source of information on the chemical composi-

* Corresponding author.
E-mail address: oded.navon@huji.ac.il (O. Navon).
[1] Present address: Department of Earth Sciences, Durham University, Durham DH1 3LE, UK.

0016-7037/$ - see front matter © 2006 Elsevier Inc. All rights reserved.
doi:10.1016/j.gca.2006.10.008

tion and on the source and evolution of the fluids from which the diamonds grow. Such inclusions are found in cubic fibrous diamonds, in the fibrous coat surrounding octahedral diamonds, and as internal clouds in the center of octahedral diamonds (Navon, 1999). The inclusion-bearing zones are populated by millions of sub-micrometer inclusions that are isolated from each other by the diamond matrix.

Fourier transform infrared (FTIR) spectroscopy of micro-inclusion-bearing diamonds indicates the presence of silicates, carbonates, and apatite, along with water, carbonate and minor molecular CO_2 (Chrenko et al., 1967; Navon et al., 1988; Zedgenizov et al., 2004; Shiryaev et al., 2005a). Transmission electron microscopy (TEM) imaging and analysis reveals that the mineral phases are present as multiphase assemblages in individual micro-inclusions (Lang and Walmsley, 1983; Guthrie et al., 1991; Walmsley and Lang, 1992a,b; Klein-BenDavid et al., 2006). Assemblages of either silicate-carbonate or halide-carbonate mineralogy, both with accessory apatite, are found together with low electron-density material (most probably a hydrous solution).

Due to their sub-micrometer size, electron probe micro-analysis (EPMA) records the bulk composition of individual micro-inclusions. While the micro-inclusions in individual diamonds are relatively uniform in composition, an inter-diamond comparison reveals a wide range of compositions between three end-members (Fig. 1): (a) a silicic end-member rich in water, Si, Al, and K; (b) a carbonatitic end-member rich in carbonate, Mg, Ca, Fe and K and (c) a saline end-member rich in water, Cl and K. Intermediate compositions between the carbonatitic and silicic components were found in fibrous diamonds from Zaire, Botswana, Brazil and Siberia (Navon et al., 1988; Schrauder and Navon, 1994; Shiryaev et al., 2005a; Klein-BenDavid and Logvinova, Unpublished data). Saline inclusions with minor carbonates were found in a fibrous Canadian diamond and in cloudy diamonds from South-Africa (Izraeli et al., 2001; Klein-BenDavid et al., 2004). No intermediate compositions between the saline component and the silicic component were detected. We use the term "saline" instead of "brine", as used by Izraeli et al. (2001), to indicate that all these fluids are dominated by chlorine and alkalies rather than by water.

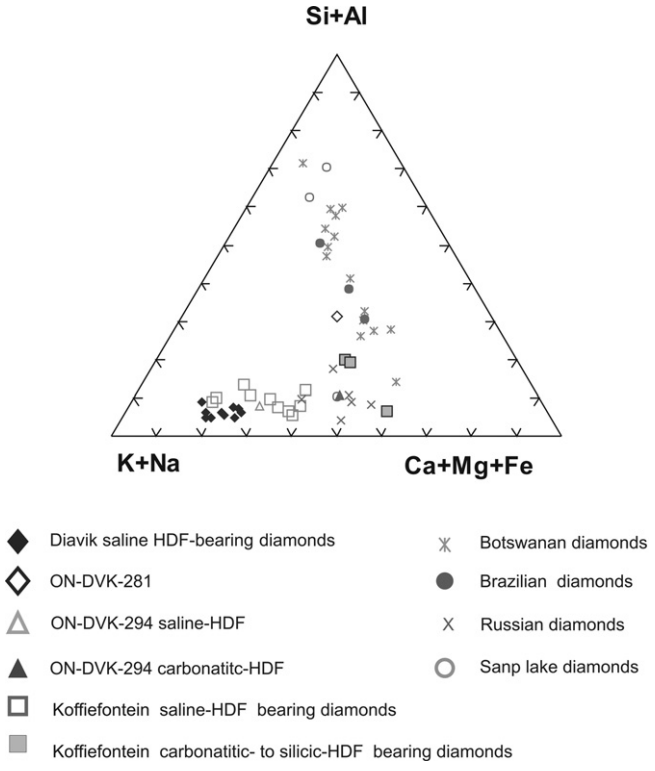

Fig. 1. The bulk composition of the micro-inclusions as detected by EPMA. The triangle presents the molar proportions of the major elements (except for Ti, Cl, and P). Data from: Jwaneng, Botswana (Schrauder and Navon, 1994); Diavik, Canada (This study and Klein-BenDavid et al., 2004); Snap-lake, Canada (Klein-BenDavid and Logvinova, unpublished data); Koffiefontein, South-Africa (Izraeli et al., 2001); Brazilian placers (Shiryaev et al., 2005a) and various mines from Russia (Logvinova et al., 2003; Klein-BenDavid and Logvinova, unpublished data).

The multi-phase assemblages observed using TEM along with the uniform EPMA analyses of the micro-inclusions in individual diamonds and the detection of water and carbonate by IR indicate that the micro-inclusions trapped homogenous fluids and that the detected minerals are secondary phases that grew during cooling, leaving a residual, volatile rich, low-density fluid. At the pressures and temperatures of the diamond stability field, many systems that carry silicate melts, carbonatitic melts and hydrous fluids, are beyond a second critical point and are fully miscible (Wyllie and Ryabchikov, 2000; Kessel et al., 2005). Thus, it seems that the fluids were trapped as uniform, highly concentrated, high-density fluids (HDF) that are similar to sub-critical melts, but may carry higher volatile content. One must distinguish between the HDF initially trapped in the inclusions and the remnant low-density fluid that is left in the micro-inclusions after the secondary mineral phases crystallized from the HDF during cooling.

Other, more reducing growth environments were suggested for both fibrous and non-fibrous diamonds. Two examples are diamond growth in a sulfide-rich melt environment (Bulanova, 1995; Sobolev et al., 1997; Bulanova et al., 1998; Klein-BenDavid et al., 2003) or from reduced carbon fluids (Tomilenko et al., 1997).

Some micro-inclusions trap minerals. In these cases the crystalline phase dominates the composition of the inclusion that may also include variable amounts of fluid (leading to mixing arrays between the two compositions, cf. Izraeli et al., 2004). Olivine, orthopyroxene, clinopyroxene, garnet, chromite, mica and carbonate were reported in cloudy and fibrous diamonds from South-Africa, Canada and Russia (Tal'nikova, 1995; Izraeli et al., 2004; Klein-BenDavid et al., 2004; Zedgenizov et al., 2004; Klein-BenDavid et al., 2006).

In spite of the wide range of major-element compositions spanned by the HDFs, they also share many similarities.

As mentioned above, the micro-inclusions in diamonds from Botswana, Zaire, South-Africa, Brazil, Russia and Canada fall along the same compositional arrays. Similar trace elements abundance ratios and REE patterns were found in Botswanan diamonds carrying a range of carbonatitic to silicic HDFs (Schrauder et al., 1996). Turner et al. (1990) found uniform Ar–K–Cl ratios in a suite of fibrous diamonds from Zaire, and halogen ratios (i.e. I/Cl and Br/Cl) in fibrous diamonds from Zaire, Botswana, Russia and Canada are mostly uniform and similar to asthenospheric values ($Br/Cl = 1.74 \pm 0.18 \times 10^{-3}$; $I/Cl = 22 \pm 3.4 \times 10^{-7}$, Burgess et al., 1998; Johnson et al., 2000; Burgess et al., 2002). Moreover, relative to the wide range of carbon isotopic composition of the general diamond population (−38.5‰ to +5‰, Cartigny, 2005), fibrous diamonds display a narrow range ($\delta^{13}C = -4.9‰$ to $-8.1‰$), close to the mantle values (Boyd and Pillinger, 1994; Boyd et al., 1994; Cartigny et al., 1998). The same is true for N isotopes; $\delta^{15}N$ values of fibrous diamonds span a narrow range (0‰ to −10‰), close to the mantle values (Cartigny, 2005). An asthenospheric noble-gas isotopic signature ($^3He/^4He = 1$–7 Ra, $^{40}Ar/^{36}Ar = 11{,}000$–$35{,}000$) was found in fibrous diamonds from Africa (Burgess et al., 1998; Wada and Matsuda, 1998).

Many of the characteristics of the HDFs are also typical in kimberlites. For example, like HDFs, kimberlites also show extreme enrichment in highly incompatible elements, steep REE patterns, high volatile contents, and carbon isotopic composition that is close to the mantle value of −5‰ (Mitchell, 1986; Le Roex et al., 2003; Kamenetsky et al., 2004). We will argue that these similarities may reflect a derivation from a similar source and by a similar mechanism.

Here we report the composition of 237 micro-inclusions in 11 diamonds from the Diavik mine in Lac de Gras, Slave Craton, Canada. The composition of an additional diamond from the Diavik mine, ON-DVK-294, was published earlier (Klein-BenDavid et al., 2004) and are discussed here in the context of the whole group. Micro-inclusions in one diamond contain fluids with compositions that are intermediate between the carbonatitic and silicic end-members. All of the other diamonds fall on the other array towards the saline end-member. These results along with published data from other locations are used to construct a model for the formation of diamond-forming fluids and their evolution within the mantle.

1.1. Lac De Gras kimberlites, diamonds and mineral inclusions

The Diavik mine is located at the center of the Slave craton beneath the shallow waters of Lac de Gras just off East Island and is composed of four high-grade kimberlites (A154 North, A154 South, A418 and A21). The kimberlites are intruded into granitoids and micaceous meta-sediments of Achaean age (Graham et al., 1999). Griffin et al. (1999) suggested that the lithospheric mantle underneath the central Slave Craton extends down to approximately 220 km.

Over 150 pipes have been identified in the Lac De Gras area. Most of them are Cretaceous to Paleocene in age (Heaman and Kjarsgaard, 2000; Creaser et al., 2004). The kimberlites are small (<2000 m^2) and steep sided relative to South-African kimberlites. A quarter of the kimberlites carry macro-diamonds. Color and morphology were published for diamonds from the neighboring Ekati kimberlites. The three most common groups are white-octahedral, brown octahedral, and fibrous diamonds (Gurney et al., 2004). The mineral inclusions found in pipes in the Lac de Gras area belong to the peridotitic, eclogitic, and super-deep parageneses with varying amounts in the different pipes (Chinn et al., 1998; Davies et al., 1999, 2004; Tappert et al., 2005).

2. The diamonds

We studied 12 diamonds from the Diavik mine. Nine of the diamonds are from pipe A154S, diamond ON-DVK-272 is from pipe A154N, and diamond ON-DVK-269 is from pipe A418. The 12th diamond, ON-DVK-294 is discussed in Klein-BenDavid et al. (2004) and is from the general Diavik production.

The diamonds weigh between 15 and 180 mg and their diameters are between 3 and 5 mm. However, six of the diamonds are broken fragments of larger diamonds of an unknown size. Five of the diamonds have an octahedral external habit, four of them are cubic in shape, and two have external habits that could not be determined.

Ten of the diamonds display similar internal structures. These diamonds have a transparent octahedral core surrounded by an opaque gray fibrous coat (Fig. 2a). Cathodoluminescence (CL) images of the diamond slabs were used as maps of the diamonds' internal structure. The octahedral cores of these diamonds have zoned CL images, revealing the core growth history. The micro-inclusion rich zones are commonly characterized by featureless, low-intensity luminescence. One diamond, ON-DVK-281, is a gray, relatively opaque, fibrous cube about 63.3 mg in weight and 5 mm in size (Fig. 2b). The slab cut from this diamond displays concentric zones of variable inclusion density, but no transparent core. This zoning is also reflected in the CL image of this diamond (Fig. 2c).

3. Methods

3.1. Sample preparation

All diamonds were polished into 0.5–1.5 mm thick slabs with two parallel faces. One diamond, ON-DVK-281, was laser-cut into a slab. The diamonds were cleaned using HF (60%) and HNO_3 (69%), and rinsed in distilled water and ethanol prior to analysis in order to remove all organic and inorganic material exposed on their surfaces. The diamonds were carbon-coated prior to EPMA analysis

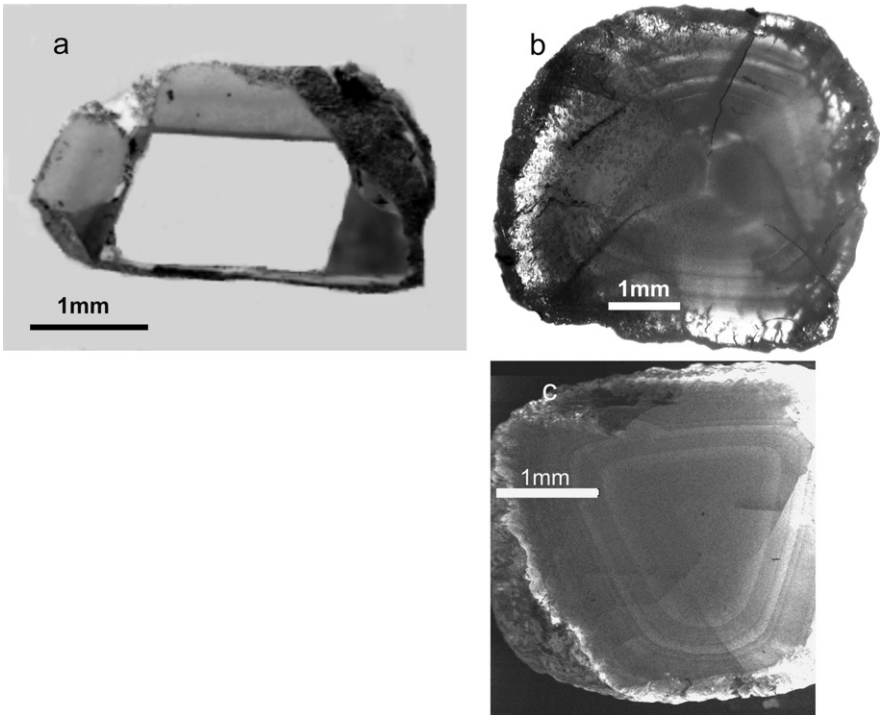

Fig. 2. Photomicrographs and a cathodoluminescence (CL) image of two diamonds from Diavik. (a) A photomicrograph of diamond ON-DVK-272. The diamond exhibits a transparent core surrounded by a fibrous, opaque, gray coat. (b) A photomicrograph of diamond ON-DVK-281. The diamond is a fibrous cube; zones of different micro-inclusion density are visible. (c) Cathodoluminescence image of diamond ON-DVK-281, the image displays concentric zoning similar to the zoning observed in b.

and CL imaging, and were gold-coated for secondary-ion mass spectrometry (SIMS) analysis.

3.2. FTIR spectroscopy

Transmission spectra were collected though the polished sections of the diamonds, using a Bruker IRscope II microscope coupled with a Nicolet 740 FTIR spectrometer (Glowbar source, KBr beamsplitter, MCT detector, He-Ne laser). Spectra were recorded with a resolution of 4 cm^{-1} in the range 600–4000 cm^{-1} though apertures of 100–300 μm in diameter. Three spectra were collected in the sample chamber of the Nicolet 740 FTIR spectrometer using a MCT detector of a wider spectral range of 400–4000 cm^{-1}, though apertures of 1–1.5 mm in diameter.

Due to the high number density of inclusions, the fibrous coats are opaque except at the core-coat boundary, which is commonly oblique to the polished surface. The core carries no inclusions, thus subtracting the diamond and nitrogen bands and correcting for baseline yields a spectrum of the absorption due to the micro-inclusions. Since EPMA analyses show uniform composition of the micro-inclusions in individual diamonds, we expect the FTIR spectral bands to represent the absorption by the micro-inclusions throughout the coat. The bands found most commonly are those of water and carbonate. The carbonate/(carbonate + water) molar ratio of the material trapped in the micro-inclusions is estimated using the maximum height of absorption bands of water and carbonate at 3420 and 1448 cm^{-1}, respectively, and the absorption coefficients given by Navon et al. (1988).

Nitrogen concentration and aggregation states in the diamond matrix are calculated based on the formulation given by Woods et al. (1990) using a computer program supplied by D. Fisher (DTC Research, Maidenhead). A ±10% error is estimated for the nitrogen concentration. However, the spectra for most diamonds are collected at the core-coat boundary; as a result, the values are an integrated average of both zones.

3.3. Electron probe analysis

Individual, shallow, subsurface micro-inclusions are detected using back-scattered electron images generated using a JEOL JXA 8600 electron probe. Individual inclusions are analyzed using a focused 15 keV, 10 nA electron beam. X-rays are collected for 100 seconds using a Pioneer-Norvar energy-dispersive spectrometer (EDS). The spectral data is reduced using the PROZA correction procedure supplied by Noran (Bastin and Heijligers, 1991) to yield the relative abundances of Si, Ti, Al, Fe, Mg, Ca, Ba, Na, K, P, Sr (S), and Cl. Fluorine was not measured as its concentration in most of the analyzed micro-inclusions was below the level of detection. Where present, it was due to remains of the HF leaching into exposed inclusions and imperfect rinsing.

Each EPMA analysis records a single micro-inclusion. As neighboring micro-inclusions are commonly separated by approximately 1 μm thick diamond matrix (Klein-Ben-David et al., 2006) and as only large, and hence relatively rare micro-inclusions are detected by EPMA, it is unlikely that analyses average multiple micro-inclusions.

The inclusion volume is considerably smaller than the volume activated by the electron beam. Moreover, about 30% of the micro-inclusion is filled by low electron-density elements (in water and carbonate), thus totals in this study are, on average, only 3.9 ± 2.1 wt%. In translating counts to weight percentages, the program assumes that the difference to 100% consists of carbon. Later, totals are renormalized to 100% (on a carbon, water- and carbonate-free basis). Izraeli et al. (2004) demonstrated that in spite of the low totals, the precision is good (about 10% relative) and the estimated accuracy is better than 15% for the major elements in the inclusions. Much of the uncertainty in the average composition of individual diamonds is due to real chemical variability between the various micro-inclusions.

Cathodoluminescence images are collected using the Gatan MiniCL attached to the EPMA. The electron beam acceleration voltage used is 25 keV. The images reflect total light intensity at the wavelength range between 180 and 700 nm.

3.4. Secondary-ion mass spectrometer (SIMS) analysis

Carbon and nitrogen isotopic compositions and N concentrations were determined along a cross-section in three of the diamonds (ON-DVK-276, ON-DVK-281 and ON-DVK-294), each carrying, a distinct fluid composition: saline, carbonatitic-silicic and carbonatitic-saline. Analyses were carried out using a Cameca 6F SIMS with a Cs^+ source (Hauri et al., 2002). Carbon isotopes were measured as C^- ions and determined using extreme energy filtering; the total uncertainty in $\delta^{13}C$ (accuracy + precision) is $\pm 0.4‰$. $\delta^{13}C$ values were calculated relative to a diamond working standard with composition of $6.51 \pm 0.1‰$ and reported relative to Pee Dee Belemnite (PDB) standard.

Nitrogen abundance and isotopic composition ($\delta^{15}N$) were measured as CN^- ions at a high mass resolving power with no energy filtering (50 eV bandpass). The total uncertainty for the nitrogen isotopic composition (accuracy + precision) is better than $\pm 4‰$. The error in the estimation of the N abundance is ±10%. The nitrogen isotopic ratios were calculated relative to working diamond standards and reported assuming an atmospheric $^{15}N/^{14}N$ ratio of 0.003676 (Hauri et al., 2002).

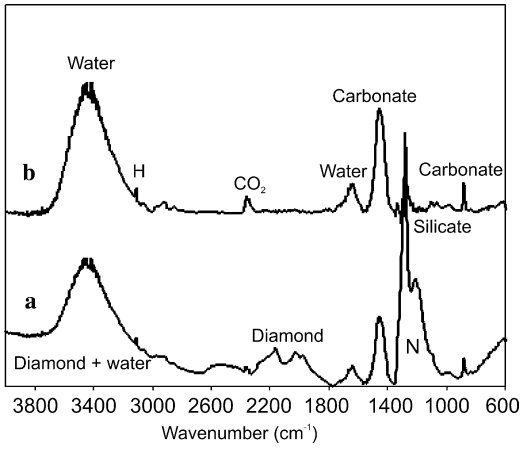

Fig. 3. IR spectra of the saline-HDF-bearing diamond ON-DVK-272. (a) The recorded spectrum is dominated by typical diamond bands at 1700–2700 cm^{-1}. The bands between 900 and 1370 (N) are typical pure type IaA spectrum due to nitrogen centers in the diamond lattice. (b) Residual spectrum after subtraction of the diamond and nitrogen bands and baseline correction. The main absorption bands are those of carbonate (880, 1448 cm^{-1}) and water (1640, 3420 cm^{-1}) in the inclusions, and hydrogen (3107 cm^{-1}) in the diamond matrix. Minor bands at 1101, 1071, 983 cm^{-1} are due to silicate absorption. The band at 2850 and 2920 cm^{-1} are attributed to organic contamination on the sample surface.

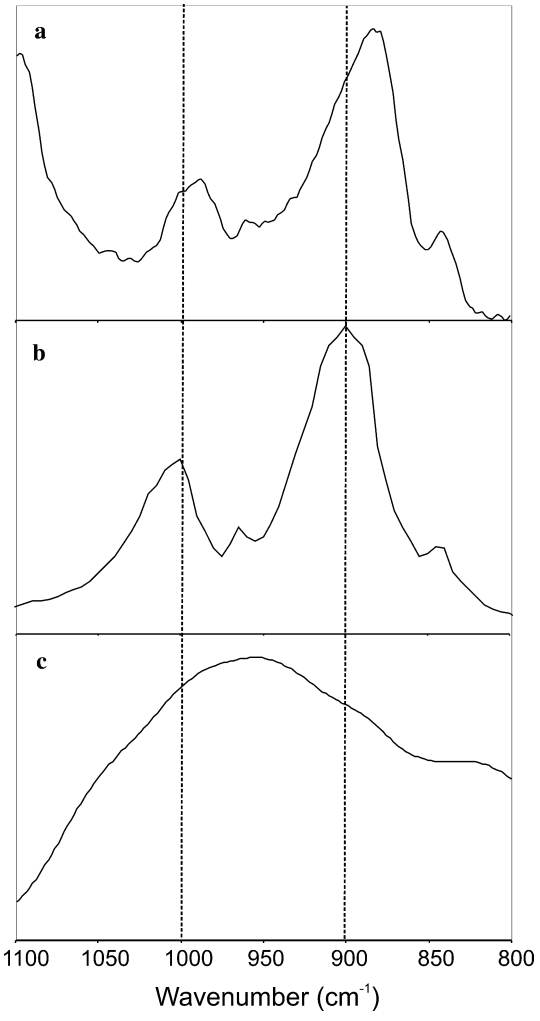

Fig. 4. (a) IR spectrum of diamond ON-DVK-276 reveals bands at 842, 884, 960, 987, 1008 cm^{-1}. (b) IR spectrum of olivine (after Farmer, 1974). (c) IR spectrum of E-phase (Mernagh and Liu, 1998; Mernagh, personal communication).

4. Results

4.1. FTIR spectroscopy

All diamond spectra are of type IaA commonly attributed to pairs of nitrogen atoms and interpreted as indicating a short residence time in the mantle. Nitrogen concentrations in the cores are 130–450 ppm and are lower than those obtained at the core-coat boundary, allowing estimation of the minimum nitrogen content for the coats to be 250–600 ppm. The main bands due to absorption by the material in the micro-inclusions are those of carbonate and water (Fig. 3). The centers of the carbonate main bands are at 1448 ± 3 and $880 \pm 1\ cm^{-1}$. The position of these bands is compatible with the dolomite and ankerite spectra. TEM analysis of inclusions in ON-DVK-272 revealed intermediate compositions between dolomite and ankerite (Klein-BenDavid et al., 2006), supporting this identification as carbonates. The spectrum of ON-DVK-283, displays bands at 721, 871 and 1420 cm^{-1}. These band locations are significantly different from those of the other spectra and indicate a different carbonate composition; however, the EPMA bulk analyses of micro-inclusions in this diamond are inseparable from the other saline-HDF bearing Diavik diamonds. The water main bands are wide and centered at 1640 and 3420 cm^{-1}. The calculated carbonate/(carbonate + water) molar ratio ranges between 0.13 and 0.39.

The spectrum of diamond ON-DVK-281 reveals bands at 460, 832, 1000, 1020, 1072 and 1095 cm^{-1}. Klein-BenDavid et al. (2006) combined IR and TEM data and attributed these bands to silica-rich mica, intermediate between phlogopite and Al-celadonite. Additional bands at 877 cm^{-1} and at 576 and 607 cm^{-1} are attributed to carbonates and apatite, respectively, which coexist with the mica in the micro-inclusions.

The spectrum of diamond ON-DVK-276 displays bands at 842, 884, 987 cm^{-1}, a small peak at 960 cm^{-1}, and a shoulder at 1008 cm^{-1}. The band locations show some similarities to the spectrum of olivine (Fig. 4a–c).

A minor band at $1010 \pm 4\ cm^{-1}$ appears in eight of the diamond spectra. An additional peak at $950 \pm 1\ cm^{-1}$ appears in seven spectra. Four spectra reveal minor bands between 840 and 848 cm^{-1}. Theses peaks are typical of silicate minerals or melts. No specific identification is possible.

Table 1
$\delta^{13}C$, $\delta^{15}N$ and N concentration measured using SIMS in diamonds ON-DVK-276, ON-DVK-281 and ON-DVK-294

Diamond	Analysis number	N[a] (ppm)	$\delta^{13}C$[b]	$\delta^{15}N$[c]	Remarks
ON-DVK-276	#1	969	−4.5	−35	Core
	#2	1098	−4.5	−34	Core
	#3	1280			Core
	#4	1447	−5.7	−2	Transition
	#5	1320	−6.0	−9	Coat
	#6	1267			Coat
	#7	1315	−4.9	−6	Coat
	#8	1275			Coat
ON-DVK-281	#1	904	−7.5	−15	Center—Fibrous cube
	#2	911			Fibrous cube
	#3	944	−8.6	−14	Fibrous cube
	#4	938			Fibrous cube
	#5	879	−11.0	−11	Fibrous cube
	#6	898			Fibrous cube
	#7	986	−9.6	−16	Fibrous cube
	#8	978			Fibrous cube
	#9	1016	−9.9	−14	Fibrous cube
	#10	1070	−10.5	−16	Rim—Fibrous cube
ON-DVK-294[d]	#1	1412	−6.0	−16	Core
	#2	1315			Core
	#3	1079	−5.2	−12	Core
	#4	669			Inner cavity rich zone
	#5	708	−8.9	−3	Inner cavity rich zone
	#7	679			Inner fibrous zone
	#8	772	−8.6	−2	Inner fibrous zone
	#9	748	−8.1	−4	Outer cavity rich zone
	#10	915	−12.8	−4	Outer fibrous zone
	#11	628			Outer fibrous zone
	#12	660	−11.4	−5	Outer fibrous zone

[a] The estimated error for the N concentration is ±10%.
[b] The estimated combined error for the $\delta^{13}C$ values is ±0.4‰.
[c] The estimated combined error for the $\delta^{15}N$ values is ±4‰.
[d] From Klein-BenDavid et al. (2004).

4.2. SIMS results

SIMS analyses were conducted along radial profiles in three of the diamonds: ON-DVK-276, ON-DVK-281 and ON-DVK-294 (Table 1). The $\delta^{13}C$ values of the fibrous zone of diamond ON-DVK-276 fall between −4.9‰ and −6‰ and are within the known range of fibrous diamonds (−4.9‰ to −8.1‰, Boyd and Pillinger, 1994; Cartigny et al., 2003). The $\delta^{13}C$ values of the fibrous zones of diamonds ON-DVK-281 and ON-DVK-294 are low (−8.5‰ to −12.8‰) and exceed the known range. Klein-BenDavid et al. (2004) have shown that a sharp change in the isotopic composition in ON-DVK-294 is associated with the transition from a saline to a carbonatitic HDF, suggesting that the highly negative values recorded in the outer part of this diamonds (−11‰ to −13‰) reflect the isotopic composition of the carbonatitic HDF. No clear pattern could be identified in the radial variation of the other two diamonds.

The HDF in ON-DVK-294 is more carbonatitic than the other Diavik diamonds. Compared to other carbonatitic HDF it is unique in its high content of Na and Ba (see Section 4.3 below). However, the silicic-carbonatitic HDF in ON-DVK-281 is similar in its chemical composition to HDFs found in diamonds from Brazil and Botswana that yielded normal isotopic values when analyzed at the same laboratory (Shiryaev et al., 2005a; Klein-BenDavid and Hauri, unpublished data). At present we can offer no explanation to the highly negative $\delta^{13}C$ of the two diamonds.

The nitrogen isotopic composition ($\delta^{15}N$) of the fibrous zones in two diamonds is similar to the known range for fibrous diamonds (0‰ to −12‰; Cartigny et al., 2003; Cartigny, 2005) however, the composition of ON-DVK-281, exceeds this range and has a $\delta^{15}N$ composition of −11‰ to −16 ‰. It is worth mentioning that although the $\delta^{15}N$ of the fibrous zone of diamond ON-DVK-276 is within the expected range, its core yielded extremely low $\delta^{15}N$ values of −34‰ to −35‰, much lower than the published range on $\delta^{15}N$ composition in diamonds (+15‰ to −25‰) (Cartigny et al., 2003; Cartigny, 2005). Again, no clear radial pattern was identified. We do not discuss these isotopic data further.

The N concentrations in the fibrous zones are in the range of 630–1320 ppm. These values are higher than the minimal estimation from IR, and are in agreement with the expected nitrogen concentrations in fibrous diamonds (Cartigny et al., 2003; Cartigny, 2005).

4.3. EPMA results

Two hundred and thirty-seven inclusions were analyzed in the fibrous zones of the 11 diamonds. Ten of the diamonds are rich in the saline component. The 11th, ON-DVK-281, contains inclusions with compositions that range between the carbonatitic and silicic HDF. Diamond ON-DVK-294 bridges between the saline composition and the more carbonatitic compositions known from other locations (Klein-BenDavid et al., 2004). Table 2 presents the composition of a representative inclusion together with the average composition of the micro-inclusions in each of the diamonds. Diamond ON-DVK-276 also contains mineral micro-inclusions; their composition is presented in Table 3.

4.3.1. Inclusions containing saline to carbonatitic HDFs

The compositions of the micro-inclusions in ten of the diamonds fall within a narrow range, intermediate between the carbonatitic and the saline end-members. The most abundant elements are Cl, K and Na. However, while K and Cl exhibit a clear positive correlation (Fig. 5a), Na has a negative correlation with Cl (Fig. 5b). Magnesium, Ca, Fe and Ba correlate positively with each other (not shown) and their total molar content correlates negatively with Cl (Fig. 5c) and positively with Na.

The carbonate content in the HDF may be constrained using the EPMA results. We assume that the charge of Ti, Ca, Mg, Fe, Ba, Na and K is balanced by chloride, phosphate, carbonate and silicate ions, and that Si and Al are associated with Mg, Fe and K in proportions that are typical of mica (Izraeli et al., 2004; Klein-BenDavid et al., 2004). Under these assumptions, we can estimate the molar carbonate content as:

$$CO_3^{2-} = 2Ti^{4+} + Ca^{2+} + Mg^{2+} + Fe^{2+} + Ba^{2+} + 0.5Na^{+} + 0.5K^{+} - 0.5Cl^{-} - 1.5PO_4^{3-} - SiO_4^{4-}$$

If this is done, then the water content may also be estimated based on the carbonate/(carbonate + water) ratio determined by FTIR. The results allow us to calculate the weight fraction of the various components in the Diavik HDF. On average, halides (and their associated K and Na) account for approximately 47 wt%; carbonates (with the associated Mg, Fe, Ca, Ba and Na) for about 31 wt%; silicates 8% and water 14%. In molar proportions, the average composition of the Diavik HDFs is: $K_{24}Na_{16}Ca_{4.4}Mg_{4.2}Fe_{3.7}Ba_{3.9}Si_{2.9}Al_{0.9}O_{10}Cl_{38}(CO_3)_{15}(H_2O)_{48}$. The low water content (about 1 water molecule for each pair of positive and negative ions), the high K/Na ratio and the association with carbonates distinguish this HDF from low pressure brines and from saline melts associated with porphyry deposits, skarns, and greisens (Roedder, 1992).

We estimate the compositions of the most saline HDF in the Diavik diamonds as: $K_{38}Na_{7.7}Ca_{1.8}Mg_{1.6}Fe_{1.5}Ba_{1.9}SiO_{3.1}Cl_{46}(CO_3)_{5.5}(H_2O)_{56}$ using a carbonate/(carbonate + water) ratio of 0.09. The carbonatitic end-member for the 11 Diavik diamonds is calculated for a carbonate/(carbonate + water) ratio of 0.5 and is: $K_{15}Na_{21}Ca_{6.7}Mg_{8.1}Fe_{6.2}Ba_{5.7}Si_{4.8}Ti_{1.4}Al_{1.9}O_{17}Cl_{29}(CO_3)_{29}(H_2O)_{29}$. (Figs. 5 and 6).

The projection of the saline-HDF compositions on a Si + Al, Ca + Mg + Fe + Na and K triangle shows that they all fall between the saline end-member and the carbonatitic end-member (Fig. 7a). A projection on a Cl, Ca + Mg + Fe + Na and K triangle shows that most inclu-

Table 2
The average bulk composition of micro-inclusions in individual Diavik diamonds along with a representative micro-inclusion for each diamond and the Diavik end-member compositions

Diamond number:	ON-DVK-269			ON-DVK-272			ON-DVK-275			ON-DVK-276			ON-DVK-280			ON-DVK-282			ON-DVK-283		
Pipe:	A418			A154N			A154S			A154S			A154S			A154S			A154S		
	Avg	SD	Individual inclusion[i]	Avg	SD	Individual inclusion	Avg	SD	Individual inclusion	Avg	SD	Individual inclusion	Avg	SD	Individual inclusion	Avg	SD	Individual inclusion	Avg	SD	Individual inclusion
Number of inclusions averaged	12			18			19			11			33			13			20		
Individual inclusion number			20			23			24			17			29			9			25
Total analysis[a]	3.1	1.0	3.2	3.5	1.2	3.6	3.6	1.9	9.5	4.4	1.6	4.1	3.7	2.4	2.2	4.1	1.7	5.4	3.6	1.4	3.8
wt%[e]																					
SiO_2[b,c]	4.1	2.8	3.4	3.8	1.8	3.0	5.2	1.7	3.4	2.8	0.8	3.1	3.8	1.9	3.0	2.9	1.9	3.1	4.2	1.8	4.0
TiO_2	0.3	1.1		0.3	1.2	—	0.6	1.5	—	0.8	2.2	2.0	1.6	2.1	3.8	2.0	2.1	2.1	0.3	0.8	—
Al_2O_3	0.7	1.3	—	0.9	1.2	1.6	0.7	1.2	1.8	0.5	1.1	—	3.0	12.7	—	0.7	1.3	—	0.5	0.8	—
FeO	6.1	3.2	6.5	7.5	3.0	5.9	5.9	2.8	7.4	7.1	2.4	3.7	5.5	3.6	4.1	6.6	4.1	7.3	5.9	3.7	4.5
MgO	2.3	1.7	3.1	3.9	1.6	2.4	4.5	2.1	4.9	3.83	0.8	3.2	2.2	1.7	3.8	3.0	2.4	3.7	4.0	1.7	4.4
CaO	4.8	1.5	5.3	7.5	2.3	7.2	6.4	2.2	7.1	2.5	1.8	4.1	4.0	1.8	3.2	4.8	3.0	4.9	5.6	2.3	6.4
BaO	11.8	3.9	14.8	11.7	5.5	10.5	13.4	6.4	13.9	19.0	3.0	17.6	13.3	5.4	14.4	12.2	4.9	14.8	14.6	5.2	18.2
Na_2O	9.5	1.9	10.6	8.3	2.6	6.1	11.8	2.0	9.9	11.1	2.2	13.0	13.0	4.4	14.9	8.8	2.5	10.6	11.5	2.9	12.3
K_2O	31.9	4.1	28.9	29.1	7.0	30.2	24.7	3.3	26.3	27.1	3.0	25.1	23.7	8.7	22.7	29.9	5.8	26.6	27.5	5.5	24.8
P_2O_5[d]	P			P		2.0	1.0	1.7		P			1.0	1.3		P		1.3	P		
Cl	34.2	30.3	35.3	3.8	3.1	31.9	30.7	31.8	29.3	32.4	2.8	34.6	32.1	6.2	31.8	32.8	5.5	30.3	30.0	6.5	28.7
SrO	1.5	1.8		1.9	2.0	3.6	1.7	2.1	1.2	0.2	0.6	1.4	2.0	2.0	5.4	2.2	1.4	2.1	1.4	1.8	—
Normalized to 100% molar[e]																					
Si	2.9	2.0	2.3	2.7	1.2	2.2	3.7	1.3	2.5	2.0	0.6	2.2	2.8	1.4	2.1	2.1	1.4	2.3	3.1	1.4	2.9
Ti	0.2	0.6	—	0.1	0.6	—	0.3	0.8	—	0.5	1.2	1.1	0.9	1.1	2.1	1.1	1.1	1.2	0.1	0.4	—
Al	0.5	1.1	—	0.7	1.0	1.4	0.6	1.1	1.5	0.5	0.9		2.7	11.6		0.6	1.2	—	0.4	0.6	—
Fe	3.6	1.9	3.8	4.5	1.8	3.6	31.5	1.6	4.6	4.3	1.5	2.2	3.4	2.6	2.5	4.0	2.7	4.5	3.7	2.5	2.7
Mg	2.4	1.8	3.2	4.2	1.8	2.6	4.8	2.3	5.3	3.7	1.0	3.4	2.3	1.8	4.1	3.3	2.7	4.0	4.4	2.0	4.9
Ca	3.7	1.2	3.9	5.8	1.9	5.6	4.9	1.7	5.5	1.9	1.4	3.1	3.1	1.5	2.5	3.8	2.4	3.9	4.4	1.9	5.0
Ba	3.3	1.2	4.0	3.4	1.6	3.0	3.9	2.0	4.0	5.5	1.0	4.9	3.8	1.7	4.1	3.5	1.4	4.3	4.2	1.6	5.2
Na	12.9	2.9	14.3	11.6	3.6	8.6	16.3	2.4	.14.1	15.7	2.9	18.0	18.0	5.9	20.8	12.4	3.5	15.2	16.2	3.8	17.4
K	28.5	2.9	25.6	26.7	5.6	27.9	22.6	2.8	24.6	25.3	2.6	22.8	21.4	7.1	20.9	27.5	5.0	25.0	25.3	3.5	23.2
P	0.3	0.8		P		1.2	P			P			0.6	0.8		P		0.8	P		
Cl	40.7	2.4	41.6	38.8	3.3	39.2	37.3	3.9	36.5	40.2	2.3	41.7	38.8	5.4	38.7	40.0	5.6	37.9	36.5	5.8	35.6
Sr	0.6	0.8	—	0.8	0.9	1.6	0.7	0.8	0.5	0.1	0.2	0.6	0.9	0.8	2.3	0.9	0.6	0.9	0.6	0.9	—
$CO_2/(H_2O + CO_2)$[f]	0.15			0.21			0.13			0.27			0.33			0.30			0.39		
CO_2[g]	10.4			14.9			13.9			14.4			12.0			14.1			15.7		
H_2O[h]	58.2			55.5			92.3			38.0			24.5			32.2			24.9		

Diamond number: Pipe:	ON-DVK-286 A154S			ON-DVK-287 A154S			ON-DVK-288 A154S			Average		Saline end-member[j]	Carbonatitic end-member[j]	ON-DVK-281 A154			ON-DVK-294[k] Carbonatitic HDF		Saline HDF	
	Avg	SD	Individual inclusion	Avg	SD	Individual inclusion	Avg	SD	Individual inclusion	Avg	SD			Avg	SD	Individual inclusion	Avg	SD	Avg	SD
Number of inclusions averaged	23			20			20			189				48			60		71	
Individual inclusion number			44			30			24							59				
Total analysis[a]	5.4	3.4	12.6	4.2	2.2	3.5	3.4	1.3	2.4	3.9	2.1			3.4	1.5	5.6	5.0	2.3	3.9	2.0
wt%																				
SiO_2[b,c]	3.4	1.4	3.4	3.5	1.4	3.0	5.0	1.8	6.4	4.0	1.8	1.5	5.8	27.5	3.9	31.8	9.3	2.8	6.4	2.4
TiO_2	1.1	1.8	1.6	1.3	2.5	2.4	0.7	1.8	—	0.8	1.8	—	2.3	2.3	2.1	4.5	1.0	1.7	0.8	1.5
Al_2O_3	0.8	1.2	—	0.5	0.9	—	0.6	1.3	2.4	1.1	5.6	—	2.8	3.6	1.3	4.7	1.6	1.3	0.9	1.4
FeO	6.8	2.2	7.8	5.3	3.0	5.5	5.2	2.9	3.8	6.0	2.9	1.5	5.1	12.6	2.9	12.9	7.7	2.0	6.3	3.0
MgO	3.8	2.2	4.7	5.9	1.6	4.2	5.2	1.7	5.0	3.9	2.1	2.2	9.2	6.2	1.6	5.0	18.6	2.6	9.1	2.4
CaO	5.8	2.1	6.9	7.3	2.0	4.4	6.7	1.6	6.0	5.7	2.4	6.3	20.7	14.3	3.0	14.0	13.0	3.1	8.1	2.4
BaO	13.9	3.5	16.4	11.9	5.0	15.2	13.1	4.5	15.2	13.6	5.1	2.2	5.9	2.5	3.5	—	7.7	4.2	10.2	4.6
Na_2O	12.8	3.7	8.9	13.9	3.2	13.4	10.2	2.3	13.8	11.6	3.4	5.6	13.2	3.2	1.5	1.7	15.5	2.6	17.6	4.7
K_2O	24.7	5.2	25.0	25.4	4.8	27.7	26.8	5.0	22.6	21.4	5.0	42.2	14.5	22.5	2.5	21.4	13.0	2.0	20.0	4.6
P_2O_5[d]	P			P		2.0	P			P		—	—	3.2	2.1	2.9	3.0	1.8	2.0	1.8
Cl	31.8	3.5	30.6	28.9	4.4	26.4	30.3	3.4	32.0	31.3	4.6	38.6	20.5	1.6	0.8	1.4	9.1	2.8	21.6	5.1
SrO	1.6	1.4	1.7	1.8	1.5	1.7	2.0	2.0		1.7	1.8			0.3	0.9		2.3	2.1	1.7	1.8
Normalized to 100% molar[e]																				
Si	2.4	1.0	2.5	2.5	1.0	2.2	3.6	1.2	4.4	2.9	1.3	1.0	4.8	24.9	3.7	29.0	7.2	2.2	4.6	1.8
Ti	0.6	0.9	0.9	0.7	1.4	1.3	0.4	1.0		0.5	1.0		1.4	1.6	1.4	3.1	0.6	1.0	0.4	0.8
Al	0.7	1.1	—	0.5	0.8	—	0.6	1.2	2.0	0.9	5.1		1.9	3.8	1.4	5.1	1.4	1.2	0.8	1.2
Fe	4.1	1.3	4.9	3.2	1.9	3.4	3.2	1.8	2.2	3.7	1.8	1.5	6.2	9.6	2.2	9.9	5.0	1.4	3.8	1.9
Mg	4.1	2.4	5.3	6.2	1.6	4.7	5.7	2.1	5.1	4.2	2.3	1.6	8.1	8.3	2.1	6.9	21.4	3.0	9.8	2.8
Ca	4.5	1.7	5.5	5.6	1.7	3.5	5.2	1.3	4.4	4.4	1.9	1.8	6.7	13.8	2.8	13.7	10.7	2.6	27.5	2.1
Ba	3.9	1.1	4.8	3.4	1.5	4.4	3.8	1.3	4.1	3.9	1.5	1.9	5.7	0.9	1.3	—	2.4	1.3	2.9	1.4
Na	17.6	4.7	12.9	19.1	4.0	19.2	14.3	3.1	18.5	16.1	4.5	7.7	21.1	5.5	2.6	3.0	23.2	3.6	24.4	5.1
K	22.4	4.5	23.8	22.9	4.1	26.02	24.6	4.0	20.0	24.1	4.9	38.1	15.3	26.0	2.8	24.9	12.9	1.9	18.4	3.8
P	P			P		1.2	P			0.4	0.8	—	—	2.5	1.6	2.2	2.0	1.2	1.2	1.1
Cl	38.3	3.3	38.7	34.6	4.0	33.1	37.1	2.8	37.5	37.9	4.4	46.3	28.7	2.5	1.2	2.2	11.9	3.6	26.1	4.7
Sr	0.7	0.6	0.7	0.8	0.6	0.7	0.9	0.9	—	0.7	0.8	—	—	0.2	0.5	—	1.0	1.0	0.7	0.7
$CO_2/(H_2O + CO_2)$[f]	0.22			0.36			0.19			0.26	0.09	0.09	0.50	0.27						
CO_2[g]	15.7			20.8			15.4			14.7	2.7	5.5	28.7	29.2						
H_2O[h]	54.3			36.8			64.6			48.1	21.1	55.7	28.7	78.9						

[a] Total amount of oxides and Cl measured by EPMA in wt% (the rest being mainly carbon from the surrounding diamond).

[b] All components except CO_2 and water after normalization to 100 wt%.

[c] Sulfur is present in some of the micro-inclusions at detection limit.

[d] Phosphorus is present in some of the micro-inclusions at detection limit.

[e] Water and carbonate free basis.

[f] The $CO_2/(CO_2 + H_2O)$molar ratio is calculated from the IR spectrum using absorption coefficients from Navon et al. (1988) $\varepsilon H_2O = 80$ (3420 cm^{-1}) and $\varepsilon CO_2 = 250$ (1430 cm^{-1}). CO_2 represents the CO_2 component of carbonates.

[g] The CO_2 molar content is calculated based on the assumption that: CO_2 in carbonate may be estimated as $CO_3^{2-} = 2Ti^{4+} + Ca^{2+} + Mg^{2+} + Fe^{2+} + Ba^{2+} + 0.5Na^{+} + 0.5K^{+} - 0.5Cl^{-} - 1.5PO_3 - n \cdot SiO_4^{4-}$ ($n = 1$ for all diamonds except for ON-DVK-281 where a value of 5/7 was used to fit the composition of secondary mica found in this diamond).

[h] The H_2O molar content is calculated from the CO_2 value and the $CO_2/(CO_2 + H_2O)$ ratio.

[i] A sample analysis of an individual micro-inclusion is given for each diamond.

[j] End-member compositions of the observed range.

[k] Averages were calculated separately for the saline inner part and for the carbonatitic outer part of the zoned diamond ON-DVK-294. A more detailed data set is presented in Klein-BenDavid et al. (2004) (small deviation from the averages presented there are due to the exclusion of 5 contaminated inclusions).

Table 3
The composition of four micro-inclusions from diamond ON-DVK-276. The micro-inclusions carry a Mg–Fe-silicate mineral phase and small amounts of fluid

Anaysis number	1	5	7	16	Average	SD
Total analysis[a,b] wt%	2.9	6.9	11.2	14.8	8.9	5.19
SiO_2	40.8	39.6	40.3	40.3	40.2	0.51
FeO	6.0	7.2	6.5	7.5	6.8	0.67
MgO	47.1	45.6	47.7	45.5	46.5	1.12
Na_2O	1.5	1.0	0.9	1.4	1.2	0.31
K_2O	1.7	2.8	2.4	2.2	2.3	0.43
Cl	2.9	3.9	2.2	3.1	3.0	0.70
Formula units (4 oxygen basis)[c]						
Si	1.04	1.03	1.03	1.04	1.04	0.01
Fe	0.13	0.16	0.14	0.16	0.15	0.02
Mg	1.79	1.78	1.81	1.75	1.78	0.02
Mg/(Mg + Fe)	0.93	0.92	0.93	0.92	0.92	0.01
(Mg + Fe)/Si	1.85	1.87	1.90	1.84	1.86	0.03

[a] Total amount of oxides and Cl before normalization (in wt%, the rest being mainly carbon from the surrounding diamond).
[b] All components measured by EPMA after normalization to 100 wt%.
[c] On average K, Na and Cl balance each other and they were not included in the calculation of the formula units.

sions are characterized by K/Cl > 1, with the saline end-member approaches K/Cl ≈ 1 (Fig. 7b).

4.3.2. Carbonatitic to silicic inclusions

One diamond, ON-DVK-281, carries micro-inclusions that are rich in Si, Fe, Mg, Ca and K and have a relatively homogenous composition. No clear correlations can be observed between the different components, rather they form a cluster with an average composition of $K_{26}Na_{5.5}Ca_{13.8}Mg_{8.3}Fe_{9.6}Ba_{0.9}P_{2.5}Si_{25}Ti_{1.6}Al_{3.8}Cl_{2.5}O_{81}(CO_3)_{29}(H_2O)_{79}$ for a carbonate/(carbonate + water) ratio of 0.27. This composition falls about one-third of the way between the carbonatitic and the silicic end-members (Fig. 7a). However, relative to the other Diavik diamonds, the carbonatitic component is lower in Ba and Na and is relatively rich in Ca compared to Fe and Mg (Fig. 8).

The above composition was calculated based on the composition of the secondary mineral assemblage observed using TEM (high-silica mica, apatite and dolomitic-ankeritic carbonate, Klein-BenDavid et al., 2006) and yields the modal abundance of the secondary phases. The average HDF holds 37 wt% of mica, 6 wt% of apatite, and 20 wt% of Ca–Mg–Fe carbonates. Water accounts for 16 wt% and K_2O, Na_2O and their associated carbonate, and Cl for the extra 21 wt%. The small amount of Cl may also be bounded in mica or apatite. It is hard to determine the site for K and Na. Klein-BenDavid et al. (2006) found no secondary potassium carbonate minerals in the inclusions and suggested that the alkalies remain in solution in the residual low-density fluid and are balanced by Cl and carbonate ions. If so, alkali carbonates account for 19 wt% and alkali chlorides for 2 wt%.

4.3.3. Minerals

Four micro-inclusions in diamond ON-DVK-276 have similar composition with an average of 40.2 wt% SiO_2, 46.5 wt% MgO, 6.8 wt% FeO, 3.0 wt% Cl, 2.3 wt% K_2O and 1.2 wt% Na_2O (Table 3). We interpret these compositions as reflecting the trapping of a silicate mineral phase along with small amounts of saline-HDF responsible for the low concentrations of Cl, K and Na in the analysis. The inclusions have Mg# of 0.92 ± 0.01 and (Mg + Fe)/Si ratio of 1.86 ± 0.03, somewhat lower than olivine (see discussion). Cr-diopside, chromite and a possible olivine micro-inclusion were found in diamond ON-DVK-294 (Klein-BenDavid et al., 2004).

5. Discussion

5.1. The mineral phases

The Mg# of the Mg–Fe-silicate in the four micro-inclusions of diamond ON-DVK-276, 0.92 ± 0.01, is within the range of olivine macro-inclusions in diamonds (Meyer, 1987; Harris, 1992) and in the lower layer of the slave lithosphere (Mg# of 0.92 ± 0.015; Griffin et al., 2004). However, the (Mg + Fe)/Si ratio (1.86 ± 0.03) is significantly lower than that of olivine and cannot be attributed to analytical error. For example, olivine-bearing micro-inclusions in diamonds from Koffiefontein (Izraeli et al., 2004) yielded a (Mg + Fe)/Si ratio of 2.1 ± 0.1. A similar phase with (Mg + Fe)/Si = 1.75 and Mg# = 0.92 was reported by Klein-BenDavid et al. (2003) in a fibrous diamond from the Yubileinaya mine, Siberia.

The IR spectrum of diamond ON-DVK-276 (Fig. 4a) also resembles that of forsterite (Fig. 4b), but the band locations are shifted with respect to the forsterite bands. The 900, 965 and 1000 cm^{-1} bands in the forsterite spectrum are shifted by approximately 15 cm^{-1} to 884, 960 and 987 cm^{-1} in the spectrum of ON-DVK-276. This may be an outcome of the difference in the chemical composition of the phases or the possible high internal pressure in the micro-inclusions (e.g. Navon, 1991).

Dense hydrous Mg-silicate (DHMS) may have Mg/Si < 2, the E-phase has a Mg/Si ratio of 1.8 (Kanzaki,

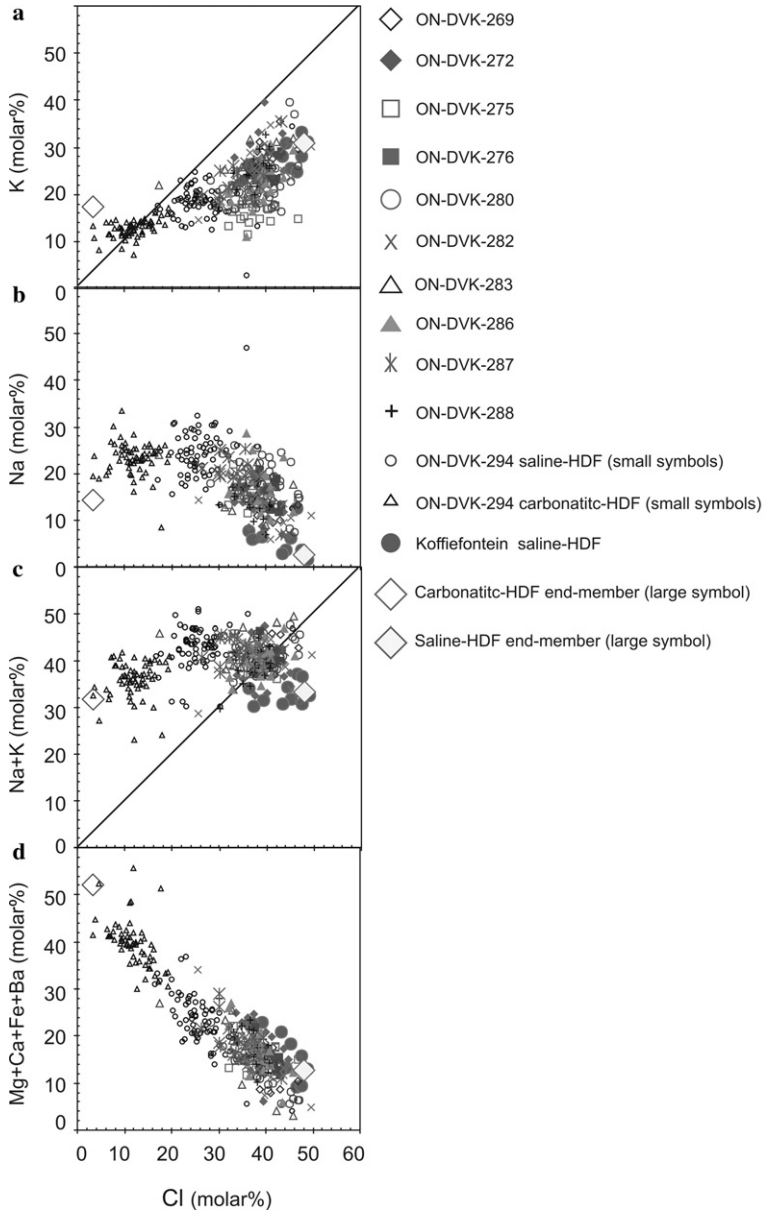

Fig. 5. The composition of individual inclusions of saline-HDFs in Diavik diamonds and sample averages for Koffiefontein diamonds. Also presented is a saline HDF end-member (solid large diamond)—the average composition of the three most saline diamonds from Koffiefontein (Izraeli et al., 2001) and a carbonatitic end-member (open large diamond)—diamond ON-UDC-239 from Udachnaya: (a) positive correlation is observed between K and Cl content. (b) Negative correlation between Na and Cl content. (c) No correlation is observed between the sum of Na and K concentrations and the Cl concentration. (d) A negative correlation between Mg + Fe + Ca + Ba and Cl contents. All concentrations are in molar proportions, water and carbonate free basis.

1991), similar to the one reported here. However, this phase exhibits a different IR spectrum (Fig. 4c) and is stable only at pressures of 13–17 GPa (Kanzaki, 1991; Komabayashi et al., 2004). Although super-deep inclusions have been encountered in Slave diamonds (Davies et al., 1999, 2004) there is no additional evidence that this diamond belongs to that paragenesis. The fluids included in the other micro-inclusions of this diamond are inseparable in composition from the fluids in the other Diavik diamonds.

Khisina et al. (2001) and Khisina and Wirth (2002) reported a hydrous-olivine phase as a nano-scale inclusion in an olivine retrieved from a peridotitic nodule from the Udachnaya kimberlite, Siberia. The (Mg + Fe)/Si ratio in this phase ranges between 1.75 and 1.66. If the Mg-silicate in diamond ON-DVK-276 represents a hydrous-olivine, it indicates a high degree of hydration of a peridotitic olivine that was entrapped in the diamond together with fluids.

5.2. The fluids

5.2.1. Saline-HDF bearing diamonds

Saline-HDFs are characterized by high K, Cl, and water contents together with variable amounts of Na, carbonate, and divalent ions (Ca, Mg, Fe and Ba); small amounts of silica are also present.

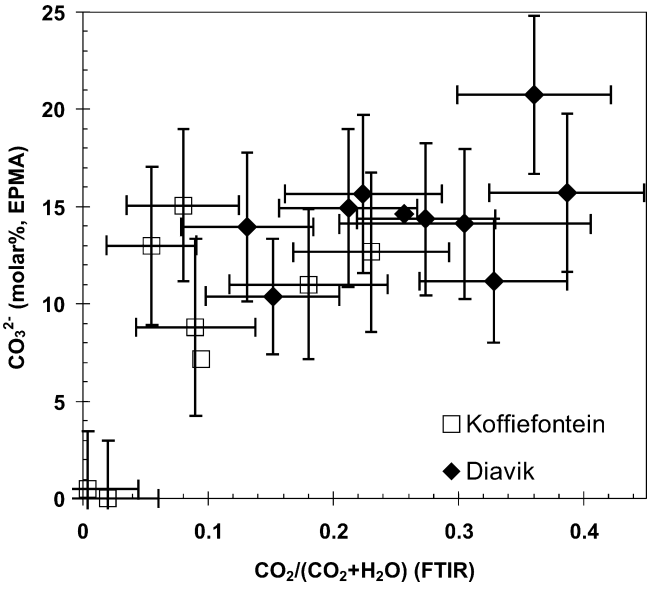

Fig. 6. The carbonate content in saline-HDF bearing diamonds from Diavik (♦, this study) and Koffiefontein (□, Izraeli et al., 2001) as calculated from EPMA analysis, versus the carbonate/(carbonate + water) molar ratio based on the FTIR spectra. Averages for each set are shown with no error bar. The carbonate molar concentration is calculated as: $CO_3^{2-} = 2Ti^{4+} + Ca^{2+} + Mg^{2+} + Fe^{2+} + Ba^{2+} + 0.5Na^{+} + 0.5K^{+} - 0.5Cl^{-} - 1.5PO_4^{3-} - SiO_4^{4-}$, (see text for details).

Diamonds containing micro-inclusions with saline to carbonatitic fluids were also found in Koffiefontein, South-Africa (Izraeli et al., 2001). These diamonds are closer to the saline end-member (up to 49 mol% Cl on a water- and carbonate-free basis) and more diluted (water/salute molar ratio up to 1.5) relative to the Diavik diamonds. Together, the two datasets define a continuous range extending from the saline end-member towards the more carbonatitic compositions of ON-DVK-294 and various carbonatitic HDFs from other locations (Figs. 1, 9 and 10). The variation diagrams in Fig. 10 also show a continuous range between the low-Cl carbonatitic composition and the high-Cl saline fluids. (Note that Fig. 10 presents only the average composition for each diamond and that if all the data are presented the arrays are continuous, as in Fig. 7).

Magnesium, calcium, and the sum of the divalent ions show a consistent negative correlation with Cl (Fig. 10a and b). The Mg# decreases constantly with increasing Cl (Fig. 10c) which can be the outcome of preferred fractionation of Mg-rich carbonates from the carbonatitic fluid (prior to its entrapment in the diamond). Alternatively, it can also be the result of fluid–rock interaction and preferred dissolution of iron, which leaves the host rocks more magnesian (see Section 5.4.5). Silica, phosphorous and aluminum show a negative correlation with Cl (Fig. 10d).

The concentrations of K and Na show opposing patterns. K slightly decreases at first and then increases with increasing Cl (Fig. 10e), while Na reaches a clear maximum at approximately 15% Cl (Fig. 10f). In the Koffiefontein diamonds the (Na + K)/Cl molar ratio is less than one and the Cl must be compensated by some divalent ions as well. In the Diavik diamonds the ratio is around one, but in some of these diamonds and even more so in ON-DVK-294 there is a surplus of alkalies (Figs. 6 and 10g), reflecting the involvement of alkali ions in the carbonatitic component.

The Na/(Ca + Mg + Fe + Ba) ratio also exhibits a maximum, with a Na increase at the expanse of both K and the divalent ions (Fig. 10h). These variations may reflect preferred fractionation of Na carbonates beginning at the intermediate stages of the saline-HDF evolution (Cl > 10 mol%). Alternatively, they may be due to fluid interaction with different local lithologies (e.g. peridotitic vs. eclogitic; Izraeli et al., 2001). Variability in the composition of the parental HFDs may also contribute to the variation in Na involvement.

5.2.2. Silicic-HDF bearing diamonds

The HDFs in diamond ON-DVK-281 lie on the array between the carbonatitic and silicic end-members defined by the Botswanan diamonds (Schrauder and Navon, 1994), close to the carbonatitic component (Figs. 1 and 9a). Similar HDFs were also found in Zairian, Botswanan, South-African, Russian, and Brazilian diamonds (Navon et al., 1988; Schrauder and Navon, 1994; Izraeli et al., 2003; Zedgenizov et al., 2004; Shiryaev et al., 2005a). In general, proceeding from the carbonatitic to the silicic end-member, the content of Si, Al, K and the water/(carbonate + water) ratio increases while the Ca, Mg, Fe, Ba and P decreases. Ti and Na are low and constant.

The Mg# of the fluids decreases from 0.56 to 0.39 with increasing SiO_2 (Schrauder and Navon, 1994; Shiryaev et al., 2005a). ON-DVK-281 has a Mg# of 0.47 ± 0.1 and falls slightly below the Botswanan correlation line and very close to the Brazilian values. The carbonate/(carbonate + water) ratio in ON-DVK-281 is also lower than that of Botswanan and Brazilian diamonds with similar SiO_2 content.

5.3. The end-members

The composition of the carbonatitic, saline and silicic end-members, can be extrapolated from the compositional arrays. These compositions can then be compared to other mantle-derived fluids and melts.

5.3.1. The saline end-member

The saline end-member is characterized by high K, Cl and water contents. Other ions such as Na, Mg, Fe and Ca are always present in small and variable proportions and are mostly balanced by the carbonate ion. The main volatile component in the saline end-member is water (Fig. 6) that constitutes up to 20 wt% of the HDF (Diavik average: 14 wt%).

Entrapment of a saline-HDF may provide an explanation for the high Br/Cl and I/Cl ratios in some Canadian

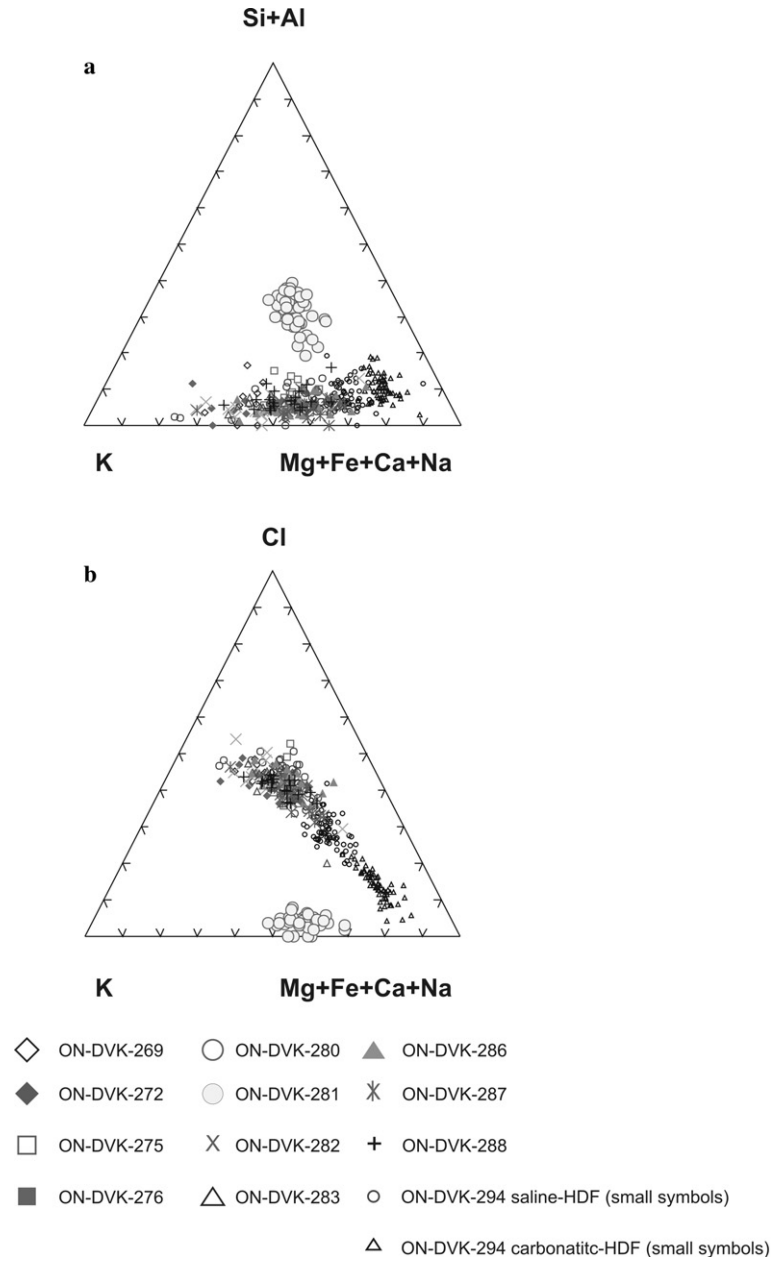

Fig. 7. The composition of all micro-inclusion in diamonds from Diavik (molar proportions). (a) a Si + Al, Mg + Fe + Ca + Na and K projection (b) a Cl, Mg + Fe + Ca + Na and K projection.

diamonds. Johnson et al. (2000) and Burgess et al. (2002) showed that, in contrast to the relatively constant ratios in diamonds from Russia and Africa, some diamonds from Canada display much higher ratios. Based on the analysis of a single saline-HDF bearing diamond, Klein-BenDavid et al. (2004) argued that the high halogen ratios may reflect the presence of saline-HDFs in such diamonds. The finding of saline HDF in 11 out of the 12 Diavik diamonds strengthens this argument. We suggest that bromine and iodine may fractionate preferably into the saline fluid, whereas Cl, as the major element of the HDF, is more limited in its enrichment and hence the high Br/Cl and I/Cl ratios.

Highly saline melt inclusions were reported in olivine crystals from the Udachnaya-east kimberlite (Kamenetsky et al., 2004). These inclusions are rich in K, Na, Cl and carbonate but contain significantly lower amounts of water (up to only 0.7 wt%) than the saline HDF included in diamonds. This is an important indication for the coexistence of highly saline melts with kimberlites. If the origin of such melts is indeed deep, it provides additional evidence for the existence of saline fluids at the source region of the diamonds.

5.3.2. The carbonatitic end-member

Carbonatitic-HDFs were encountered in diamonds from Botswana, Koffiefontein, Russia, Canada and Brazil

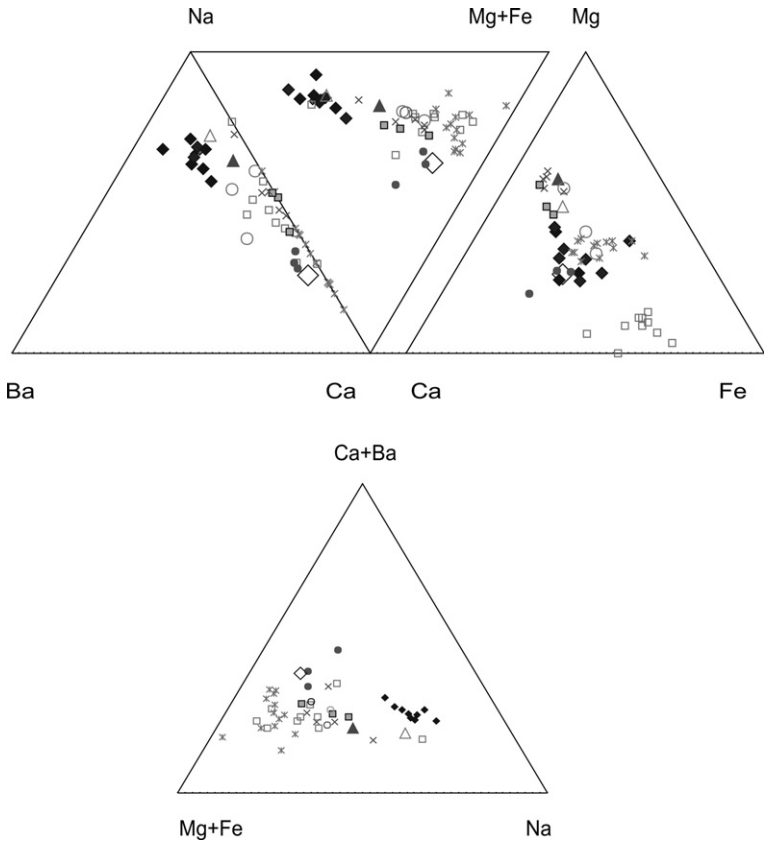

Fig. 8. The average composition of Mg, Ca, Fe, Ba, and Na in micro-inclusions in individual diamonds from various localities. See Fig. 1 for the legend to the symbols and for data sources.

(Schrauder and Navon, 1994; Izraeli et al., 2003; Klein-BenDavid et al., 2003; Logvinova et al., 2003; Klein-BenDavid et al., 2004; Zedgenizov et al., 2004; Shiryaev et al., 2005a). The carbonatitic end-member is characterized by high K, Mg, Ca, Fe, and carbonate concentrations and may contain variable but significant amounts of Na and Ba. Si is always present and its concentration is around 10 wt%. Chlorine and P occur at low concentrations (2–5 wt%) and Al and Ti are close to or at the detection level.

The carbonate/(carbonate + water) molar ratio of the carbonatitic-HDFs is high and ranges from 0.5 to 0.7, indicating that measurable amounts of water are always present in the carbonatitic diamond-forming HDF. This observation emphasizes the important role of water in catalyzing diamond growth and is in agreement with the experimental results of Pal'yanov et al. (1999, 2005) who found enhanced diamond growth from carbonatitic melts carrying more then 5 wt% of water.

The Ca/(Ca + Fe + Mg) molar ratio in carbonatitic-HDFs (0.3–0.4, Fig. 8) is lower than that of experimentally derived carbonatitic melts in equilibrium with peridotites (0.4–0.55, Gudfinnsson and Presnall, 2005; Keshav et al., 2005), or of magnesio-carbonatites (0.5–0.7, Woolley and Kempe, 1989; van Achterbergh et al., 2002); it is higher than the ratio in kimberlites and lamproites (~0.2–0.3, Wannamaker et al., 2000; Salvioli-Mariani et al., 2004; Becker and Le Roex, 2006). The Ca/(Ca + Mg + Fe) ratio of carbonatitic melts formed by melting of carbonate peridotites decreases with increasing degree of melting (Dalton and Presnall, 1998). This may indicate that the carbonatitic-HDFs are products of an intermediate degree of melting (or fluid/rock ratio) between those characteristic of carbonatitic and kimberlitic magmas. It is also possible that the high water activity substantially lowers the solidus temperature, and thus affects the Ca/(Ca + Mg + Fe) ratio (Girnis et al., 2005; Gudfinnsson and Presnall, 2005). The relatively constant Ca/(Ca + Mg + Fe) ratio in the carbonatitic HDFs supports a similar derivation mechanism of the HDFs in various locations (mostly, similar fluid/rock ratio).

The Mg# of the carbonatitic-HDFs is more variable, ranging between 0.55 and 0.85 (Fig. 10c). This range is in agreement with that of naturally occurring carbonatites (Woolley and Kempe, 1989) and somewhat lower than that found in carbonatitic melt inclusions in olivine (0.90, van Achterbergh et al., 2002).

The K_2O concentration of the carbonatitic-HDF is relatively high and constant (15–20 wt%). The K/(Na + K + Ca + Mg + Fe) molar ratio ranges between 0.17 and 0.33. In contrast, the Na concentration of the carbonatitic-HDF varies considerably (Na_2O = 2–20 wt%; Na/(Na + K + Ca + Mg + Fe) = 0.05–0.34). Both K and Na

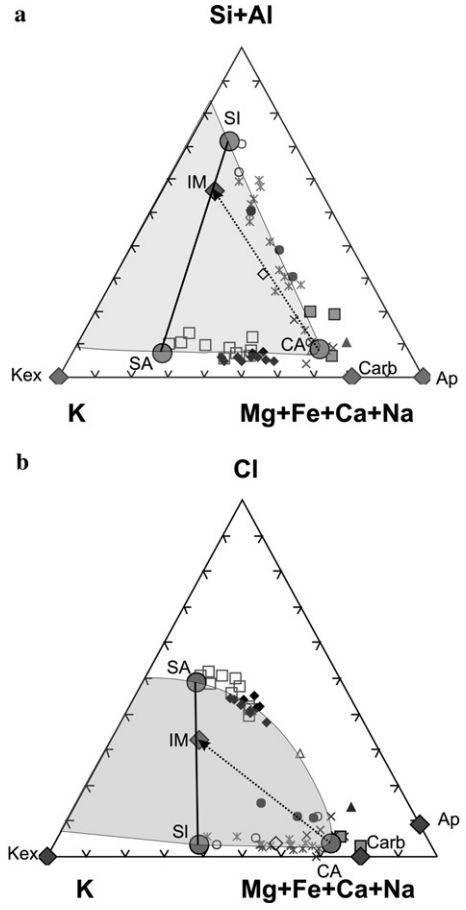

Fig. 9. Model for evolution of the HDFs. The initial carbonatitic HDF (CA) precipitates carbonate (Carb), apatite (Ap), and titanates (not shown in this figure) to produce an immiscible mixture (IM) of silicic (SI) and saline (SA) HDFs and a small excess of water (not shown) and potassium (Kex). The shaded area represents the possible immiscible region (plotted to fit the diamond analyses, see Fig. 1 for legend and sources).

are enriched relative to ferro- and magnesio-carbonatites where the total alkali content is lower than 5.5 wt% (Woolley and Kempe, 1989, water and CO_2 free basis).

5.3.3. The silicic end-member

The silicic end-member is characterized by high Si, K, Al, Ti and water contents. Carbonate is always present in the silicic component along with minor amounts of Ca, Mg, Fe, Na, P and Cl. The carbonate/(carbonate + water) molar ratio is around 0.1 (Schrauder and Navon, 1994). The estimated fraction of water in the silicic end-member is in the range of about 10 wt% (and up to 40% in diamonds from Brazil; Shiryaev et al., 2005a) and is similar to the water fraction of hydrous-silicic melts and silicic supercritical fluids at the high pressures of the diamond stability field (Schmidt et al., 2004; Kessel et al., 2005). The Al/Si and K/Si molar ratios are similar in the silicic end-member in diamonds from different locations and are 0.14–0.23 and 0.25–0.3, respectively. Comparison to high-pressure hydrous-silicic melts in equilibrium with eclogites reveals a higher Al/Si ratio and a much lower K/Si ratio, 0.25–0.3 and ~0.02, respectively (Hammouda, 2003; Schmidt et al., 2004; Kessel et al., 2005).

5.4. Chemical evolution of the fluids

The continuous arrays connecting the carbonatitic component with the saline and the silicic end-members (Figs. 1 and 9) suggest that the three fluids are genetically related. We evaluate the possible role of the following processes in the evolution of the diamond-forming fluids: (1) dissolution and melting of carbonated eclogites and peridotites, (2) cooling and crystallization of carbonates from a primary carbonatitic melt (Schrauder and Navon, 1994), (3) formation of both the silicic-HDF and the saline-HDF by immiscibility and separation of fluids formed during cooling of a parental carbonatitic melt (Perchuk et al., 2002), (4) mixing of HDFs produced under different conditions (Schrauder and Navon, 1994), (5) the modification of fluids through metasomatic interaction during percolation or flow through veins.

5.4.1. Melting of carbonated peridotites and eclogites

Carbonate-rich melts are abundant as low-fraction melts of the upper mantle, they are considered major metasomatic agents both in the oceanic and continental lithosphere and are highly rich in incompatible elements (Yaxley and Brey, 2004 and references therein). Experimental data at pressures of 1.5–5.5 GPa (Falloon and Green, 1990; Yaxley and Green, 1994; Dalton and Presnall, 1998; Yaxley, 1999; Hammouda, 2003; Yaxley and Brey, 2004) indicate that melting of carbonated peridotite and eclogites yields carbonatitic melts. Carbonated peridotites produce dolomitic primary liquids at pressures higher then 3 GPa (Wyllie and Huang, 1975; Wallace and Green, 1988; Wyllie, 1989; Sweeney, 1994; Dalton and Presnall, 1998; Girnis et al., 2005); carbonate bearing eclogitic assemblages produce calico-dolomitic melts (Nelson et al., 1988; Hoernle et al., 2002; Hammouda, 2003; Yaxley and Brey, 2004). Alkali-rich carbonatites may be produced through the melting of carbonated phlogopite peridotites or eclogites, as shown by Thibault et al. (1992) and Dasgupta et al. (2005) at 3 GPa.

Hydrous-silicic fluids may be present both as sub-solidus fluids at lower pressures and as super-critical fluids at high pressures (Wyllie and Ryabchikov, 2000; Schmidt et al., 2004; Kessel et al., 2005). Kessel et al. (2005) demonstrate that at pressures lower than 6 GPa, eclogites produces hydrous-fluids with up to 20% SiO_2 at sub-solidus conditions (700–1000 °C) and a silicic melt (<20% H_2O) at higher temperatures. Above 6 GPa the system is beyond a second critical point and full miscibility exists between hydrous-fluids and silicic melts. In a carbon-bearing eclogite such fluids also dissolve carbonates (Pal'yanov et al., 2005). Yaxley and Green (1994) and Hammouda (2003) demonstrate that upon heating, carbonate-bearing eclogite first yields a silicic melt that then evolves into carbonatitic melts with further heating. Thus, in a system

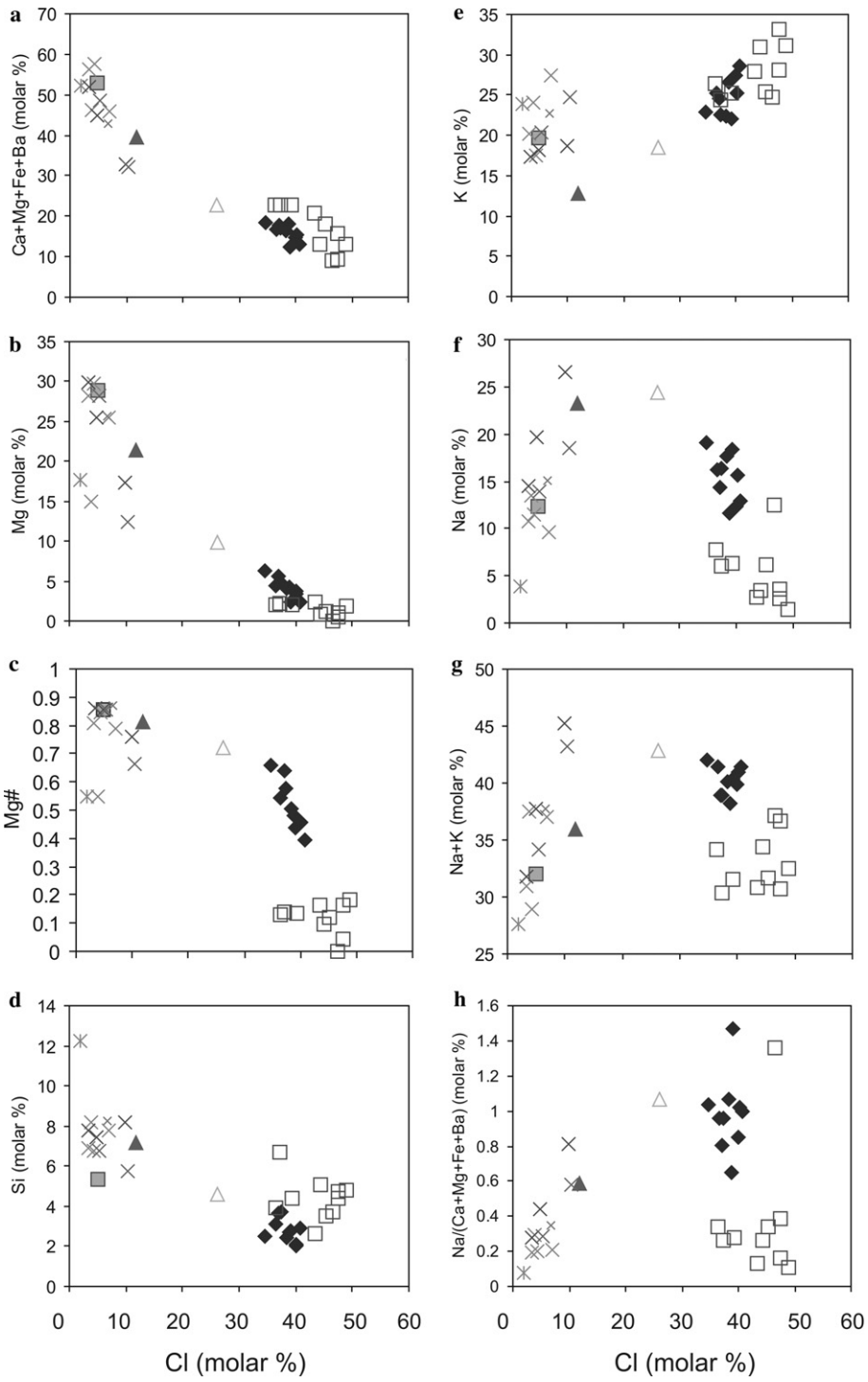

Fig. 10. Average compositions of micro-inclusion in carbonatitic to saline HDF-bearing diamonds (molar proportions): (a) the sum of the divalent ions (Ca + Mg + Fe + Ba) vs. Cl. (b) Mg content. (c) Mg#. (d) Si. (e) K first decreases and then increases with increasing Cl contents. (f) Na first increases and then decreases with increasing Cl contents. (g) Na + K. (h) The Na/(Ca + Mg + Fe + Ba) molar ratio. See Fig. 1 for the legend to the symbols and for data sources.

containing a hydrous fluid and carbonated eclogite, the carbonate concentration of the fluid increases upon heating.

It is not easy to produce saline melts in a melting scenario. Saline-melts are known from lower pressure magmatic and metamorphic systems (Roedder, 1992; Scambelluri and Philippot, 2001). They may be present at temperatures below the carbonated peridotite solidus and evolve into carbonatitic melts upon heating. Kamenetsky et al. (2004) suggested that the salt-rich inclusions in olivine

phenocryst in fresh kimberlite samples from Udachnaya, Siberia trapped a K, Na, Cl and carbonate rich melt at depth, indicating the existence of K–Cl rich fluids at the diamond source region.

Heating carbonated rocks where either hydrous-silicic or hydrous-saline fluids are present should lead to dissolution of carbonates into the fluid. Such a model can explain either of the observed compositional arrays. In the melting model the two arrays are independent, and the initial fluid should be either silicic or saline in different rocks. The finding of both eclogitic and peridotitic minerals in Koffiefontein diamonds carrying saline HDFs (Izraeli et al., 2004) excludes a model where each array evolves in a different type of host-rock.

Of greater concern is the carbon solubility of the fluids. Carbon solubility increases upon heating of hydrous-silicic melts (Pal'yanov et al., 2005) and hydrous fluids (Liu et al., 2002). Diamonds are expected to dissolve into the melt rather than precipitate from it as the melt evolves towards the carbonatitic composition and higher temperatures. Thus, a melting model is unlikely to explain the observed compositional range.

5.4.2. Crystallization of a parental carbonatitic melt

Schrauder and Navon (1994) suggest that the crystallization of carbonates from a carbonatitic melt might produce the array towards the silicic end-member. The variation diagrams they examined suggested that the carbonate must remove Ca, Mg, and Fe as well as alkalies to produce the observed array. Additional phases must be removed in order to explain the lack of enrichment with P, Ti, and Cl content. Shiryaev et al. (2005a) note that water must be removed as well in order to explain the increase in the silicate/water ratio during evolution from carbonatitic to hydrous-silicic compositions.

This process accounts only for the carbonatitic-silicic array. A different carbonate composition and an extreme fractionation is needed in order to evolve towards the saline end-member and to raise the Cl concentration from about 2 mol% in the original carbonatitic-HDF to about 48 mol% in the saline-HDF. Additional phases must crystallize in order to control the Si, Al, Ti and K concentrations. Thus, an alternative process must be invoked in order to explain the evolution of the saline HDFs and the silicate/water ratio of the silicic HDF.

5.4.3. Crystallization and liquid immiscibility

Ternary diagrams of the major ions in the different fluids (Fig. 9) reveal a wide compositional gap between the silicic HDFs and the saline HDFs. Such a gap may be the result of an immiscible separation of HDFs that evolved from a parental carbonatitic component. Perchuk et al. (2002) suggested this process by extrapolating from experimental data that documented immiscibility between a silicic melt and a K–Cl melt at pressures lower than 2.5 GPa.

Crystallization and immiscibility may be combined to form a model that can explain the two arrays. Crystallization of carbonates drives the composition of the initial carbonatitic fluid into an immiscible region where it separates into silicic and saline HDFs.

In order to drive the residual fluid into the immiscibility gap and to maintain mass balance the fractionating carbonate should be composed of about 60% Ca + Mg + Fe and 40% K + Na (Figs. 1 and 9). The negative correlation between the divalent ions and either Cl (Fig. 10a) or SiO_2 (in silicic HDFs; Schrauder and Navon, 1994; Shiryaev et al., 2005a) suggests that divalent ion carbonates precipitate from the evolving carbonatitic HDF from the initial stages of its evolution. The negative correlation between Mg# and Cl indicates preferential fractionation of Mg-carbonates (Fig. 10b and c).

Sodium concentration increases with increasing Cl content at the initial stages of the fluid evolution ($Cl < 15$ mol%), and decreases at higher Cl content (Fig. 10f). As sodium is only a minor component of the silicic HDF (Schrauder and Navon, 1994; Shiryaev et al., 2005a), we suggest that Na is first fractionated into the saline HDF, and only when its activity reaches a threshold, Na-carbonates begin to precipitate leading to a decrease in Na concentrations at $Cl > 15$ mol%. Potassium is high in both silicic and saline HDFs but must also be removed by the fractionating carbonates (Fig. 9 and 10e). The carbonatitic end-member (Schrauder and Navon, 1994) is characterized by a high K/Cl ratio (~12) and low Cl content (2 mol%). The low K/Cl molar ratio in the saline-HDF (~0.7) means that even if the saline HDF retains all of the Cl, it can only account for 7% of the original K content. The silicic end-member cannot host the extra K either. The K/Si ratio in the carbonatitic is ~2 while in the silicic end-member it is ~0.3 (Schrauder and Navon, 1994). Thus, only 15% of the original K may end up in the silicic end-member. The other ~78% of the K must be removed by another phase, most probably the carbonates, or be removed by metasomatism (see below).

Fig. 9, together with a quantitative model accounting for the volatile and the minor components, enable the estimation of the proportions of the HDFs created from the initial carbonatitic fluid. Using the end-member presented in Fig. 9 and removing carbonate apatite and titanate, we obtain a residual mix of the silicic and the saline end-members. Examining the results obtained by reasonable variation of end member composition, the carbonate–water ratio, and the carbonate and apatite composition, we found that the results are quite robust. In most scenarios, about 75 wt% carbonate, 5 wt% apatite and 1.6 wt% titanate are removed, leaving 10–11 wt% silicic HDF, 3.5–5 wt% of the saline end-member, and a small excess (~3 wt%) of water and potassium.

We suggest that crystallization and separation of immiscible fluids provide a suitable mechanism for the evolution of the HDFs. All fluids may precipitate diamonds until they consume most of their carbonate content. The extra water and perhaps K may be consumed by metasomatic reactions with the wall rock.

5.4.4. Mixing

Once all the end-members are available mixing may occur between them. Klein-BenDavid et al. (2004) and Shiryaev et al. (2005a) have shown mixing between different HDFs in the same diamond. Klein-BenDavid et al. (2004) reported a sharp but continuous transition from a saline-HDF to a more carbonatitic composition in two concentric zones of diamond ON-DVK-294 from Diavik. Shiryaev et al. (2005a) demonstrated a sharp transition from a silicic to a carbonatitic HDF in a Brazilian diamond. In both cases the sharp compositional zoning is opposite to the expected fractionation trend and probably represents fresh influx of carbonatitic fluid (similar to the recharging of fractionating crustal magma chambers by fresh batches of mafic magma). Immiscibility should prevent mixing between saline and silicic HDFs.

5.4.5. Metasomatic interaction

All the fluids found in the micro-inclusions may act as metasomatic agents. Such metasomatic interactions must affect not only the host rock but also the flowing fluids. Mass-balance calculations indicate that while the host-rock is mostly affected in its incompatible elements budget, in the fluid the major elements are more sensitive to such interaction (Navon and Stolper, 1987).

Izraeli et al. (2001) reported that in HDFs found with peridotitic minerals the Na concentrations were higher than in HDFs found with eclogitic minerals. They attributed this difference to the higher compatibility of Na in eclogitic assemblages. Alternatively, mica formation during metasomatic interaction with the wall rocks may decrease the K content of the fluid. Water would also be removed, explaining the consistent surplus in water and cations in the fractionation model discussed in Section 5.4.3.

The decrease in Mg# from carbonatitic to either silicic or saline HDFs (Fig. 10c) may also reflect a continuous interaction with the host-rocks and a partition of Fe into the fluid. The variability in the Fe content may be the result of fluid interaction with a host-rock's different mineralogy. For example, Girnis et al. (2005) suggest that the garnet/orthopyroxene ratio controls the Mg# of the fluid, with higher garnet abundances leading to lower Fe concentration.

5.4.6. The preferred model

We suggest that all HDFs are derived from parental carbonatitic fluids. Upon cooling, a parental carbonatitic-HDF crystallizes carbonates and other minor phases and drives the HDF composition into an immiscibility gap where it separates into silicic and saline HDFs. Each fluid may go on fractionating carbonates and diamonds until it consumes its carbon reserves. Metasomatic interaction may also play a role in the evolution of the fluids and mixing between evolved and fresh HDFs also occurs.

The finding of diamonds in association with veins and secondary minerals in diamondiferous xenoliths (Taylor et al., 2000; Taylor and Anand, 2004) suggests that the above processes take place during the flow of the HDFs through veins and channels in the peridotitic or eclogitic host-rocks. Thus, we envision that crystallization, fractionation, or immiscible separation take place in veins or small pockets filled with HDF, where interaction with the wall rock may be significant.

5.5. The role of fluids in diamond formation

5.5.1. Diamond synthesis

Experimental evidence supports diamond growth from carbonate bearing melts at pressures and temperatures that are similar to those recorded by diamond mineral inclusions (as low as 1150 °C and 5.7 GPa; Pal'yanov et al., 1999; Spivak and Litvin, 2004). Diamonds were also grown from compositions that are close to that of carbonatitic-silicic HDFs (Shiryaev et al., 2005b; down to 1340 °C, 6 GPa). In general, the addition of water and up to 10% SiO_2 was shown to enhances diamond growth efficiency from such melts (Shatsky et al., 2002; Pal'yanov et al., 2005).

5.5.2. The source of the fluid

All HDFs are rich in volatiles and incompatible elements. The high levels of carbonates, water, K, Ba, P, and Cl were discussed above. Highly incompatible trace elements, halogens, and rare gases are enriched by up to 10^3–10^4 of the primitive mantle values (Turner et al., 1990; Schrauder et al., 1996; Johnson et al., 2000; Burgess et al., 2002; Rege et al., 2005). Such a high level of enrichment in incompatible components requires derivation from a relatively large volume of mantle rocks (a low fluid/rock ratio).

Despite the indications of a low fluid/rock ratio, the HDFs are relatively uniform in composition (see Section 1). The observed enrichment in incompatible elements together with the relative uniformity in elemental and isotopic ratios may be explained if the fluids or their predecessors had interacted with large mantle volumes.

Khazan and Fialko (2005) have recently invoked a percolation model in order to explain the similarities in trace element patterns in kimberlites. A similar mechanism may explain the uniformity of the carbonatitic HDFs or of their predecessors.

5.5.3. Kimberlites, lamproites, and diamond-forming HDF

Both kimberlites and lamproites are derived from the diamond stability field and carry diamonds to the surface. Both are rich in water, carbonate, and incompatible elements. Kimberlites are silica-depleted and highly magnesian while lamproites are basic to ultrabasic (SiO_2 45–55 wt%), peralkaline, and ultrapotassic. Both are derived by low degrees of melting of peridotite at high pressures. Kimberlite sources carry carbonate while the lamproites probably originate from heavily metasomatized, vein-rich peridotite (Mitchell and Bergman, 1991; Foley,

1992a,b; Brey and Ryabchikov, 1994; Dalton and Presnall, 1998; Mitchell and Edgar, 2002; Girnis et al., 2005).

Diamond-forming HDFs are volatile-rich, with up to 40 wt% of water and CO_2 (in carbonates). Kimberlites have lower volatile contents, but CO_2, preserved in calcite and dolomite, accounts for an average of about 6 wt% and may reach levels of 18 wt% (Price et al., 2000), and water in serpentine, phlogopite, and secondary minerals may reach 4–8 wt% (Mitchell, 1986). Lamproites commonly contain about 5 wt% of volatiles (CO_2 and H_2O) but may contain up to 15 wt% (Wannamaker et al., 2000; Rao et al., 2004; Salvioli-Mariani et al., 2004).

Kimberlites contain less than 2 wt% of alkalies and Cl, much less than HDFs. However, Kamenetsky et al. (2004) found more then 8 wt% of water soluble material (mostly Na–K halides and carbonates) in fresh kimberlite from the Udachnaya-East kimberlite. If such levels are common but cannot be recognized due to the weathered state of most kimberlites, the K and Cl content of the kimberlitic magma at depth may be closer to that of the carbonatitic HDFs. Lamproites, on the other hand, carry elevated alkali concentrations ($Na_2O + K_2O$ up to 16 wt%) similar to these of HDFs, but with a Cl content lower then 1 wt%.

The above comparison was made between HDFs trapped and preserved under high pressure conditions and magmas that have reached upper crustal levels and may have lost volatiles during accent. Price et al. (2000) and Le Roex et al. (2003) argue that CO_2 loss is minimal. Alternatively, Brey et al. (1991) and Girnis et al. (1995, 2005) advocate the formation of kimberlites as saturated melts that degas at sub-crustal pressures. Similarly, Salvioli-Mariani et al. (2004) show a CO_2 release from lamproitic magmas at shallow pressures. Water and Cl may also be lost during degassing (Kamenetsky et al., 2004; Maas et al., 2005). If indeed volatiles and alkalies are lost during accent, then the parental magmas of kimberlites and lamproites are rich enough in these components (Brey et al., 1991) and may be parental to the HDFs as well.

The CaO/(CaO + MgO + FeO) ratio in the carbonatitic HDF is 0.3–0.4, intermediate between that of carbonatites and kimberlites or lamproites. Girnis et al. (2005) and Dalton and Presnall, 1998) showed a gradual change from a carbonatitic to kimberlitic melts with increasing degrees of melting of a carbonated peridotite (0–1%, 4–6 GPa and 1450–1650 °C). The intermediate ratios of the HDFs may represent a higher degree of partial melting relative to carbonatitic melts or fractional crystallization from kimberlitic or lamproitic melts.

Kimberlites, lamproites and diamond-growing-HDFs are all rich in incompatible elements (10^2–10^3 times the primitive mantle values) and have similar trace element abundance patterns (Schrauder et al., 1996; Navon et al., 2003; Rege et al., 2005). Still, important differences exist between these fluids, differences that can only be partially removed by degassing during ascent. For example, the extreme enrichment of the HDFs in alkalies cannot be easily accommodated with the low alkali contents of surface kimberlites. Lamproites carry more alkalies, but their high SiO_2, Al_2O_3, and TiO_2 content requires extensive fractional crystallization of the parental lamproitic melts to yield carbonatitic-HDFs. Still, the observed similarities between diamond-forming HDFs, kimberlitic and lamproitic melts and their common association with diamonds lead us to suggest that diamond-forming HDFs may originate from similar melts. Kimberlites ascend and degas, losing some of their CO_2 (Yaxley et al., 1991; Ionov et al., 1993; Yaxley and Green, 1998) and alkalies. Diamond-forming fluids evolve from similar alkali-rich melts that fractionate at high pressures.

6. Conclusions

Fluid-bearing micro-inclusions in diamonds from the Diavik mine, Canada, span much of the previously recorded compositional range of fluids trapped in diamonds. They span a continuous array between carbonatitic and saline HDFs, and part of the range between the carbonatitic and silicic end-members. Following the suggestion of Perchuk et al. (2002) we propose a model where the carbonatitic-HDFs are the parental fluids for both arrays. Divalent and alkali carbonates that precipitate from the parental carbonatitic HDF drive its composition into an immiscibility gap and the fluid separates into saline and silicic HDFs. Each component then continues to evolve separately, fractionating carbonates, diamonds, a few accessory minerals and more of the immiscible phase. All fluids may act as metasomatic agents and are probably affected by metasomatic interaction with the mantle host-rocks.

The carbonatitic-HDF evolves by fractional crystallization of an alkali-rich melt that may also be parental to kimberlites or lamproites. The carbonatitic-HDF or its predecessor parental melt percolates through relatively large mantle volumes. Local heterogeneities are mostly averaged but some are reflected in the variation of major elements of the carbonatitic end-member in each location.

Acknowledgments

We thank Diavik Mining Corporation for contributing the diamonds, Yakov Weiss, Tamar Shalev, Bill Griffin, and two anonymous reviewers for their constructive comments, and Jianhua Wang for expert maintenance of the Carnegie ion microprobe. Research was supported by the Israeli Science Foundation (ISF 90/01 to Oded Navon).

Associate editor: Martin A. Menzies

References

Bastin, G., Heijligers, J., 1991. In: Heinrich, K., Newbury, D. (Eds.), *Electron Probe Quantitation, Workshop at the National Bureau of*

Standards, Gaithersburg, Maryland. Plenum Press, New York, pp. 145–161.

Becker, M., Le Roex, A.P., 2006. Geochemistry of South African on- and off-craton, Group I and Group II kimberlites: petrogenesis and source region evolution. *J. Petrol.* **47** (4), 673–703.

Boyd, S.R., Pillinger, C.T., 1994. A preliminary-study of $^{15}N/^{14}N$ in octahedral growth form diamonds. *Chem. Geol.* **116** (1–2), 43–59.

Boyd, S.R., Pineau, F., Javoy, M., 1994. Modeling the growth of natural diamonds. *Chem. Geol.* **116** (1–2), 29–42.

Brey, G.P., Ryabchikov, I.D., 1994. Carbon-dioxide in strongly silica undersaturated melts and origin of kimberlite magmas. *Neues Jahrbuch Mineral. Monatshefte* (10), 449–463.

Brey, G.P., Kogarko, L.N., Ryabchikov, I.D., 1991. Carbon-dioxide in kimberlitic melts. *Neues Jahrbuch Mineral. Monatshefte* (4), 159–168.

Bulanova, G.P., 1995. The formation of diamond. *J. Geochem. Exploration* **53** (1–3), 1–23.

Bulanova, G.P., Griffin, W.L., Ryan, C.G., 1998. Nucleation environment of diamonds from Yakutian kimberlites. *Mineral. Mag.* **62** (3), 409–419.

Burgess, R., Johnson, L.H., Mattey, D.P., Harris, J.W., Turner, G., 1998. He, Ar and C isotopes in coated and polycrystalline diamonds. *Chem. Geol.* **146**, 205–217.

Burgess, R., Layzelle, E., Turner, G., Harris, J.W., 2002. Constraints on the age and halogen composition of mantle fluids in Siberian coated diamonds. *Earth Planet. Sci. Lett.* **197** (3-4), 193–203.

Cartigny, P., 2005. Stable isotopes and the origin of diamond. *Elements* **1** (2), 79–84.

Cartigny, P., Harris, J.W., Phillips, D., Girard, M., Javoy, M., 1998. Subduction-related diamonds? The evidence for a mantle-derived origin from coupled delta $\delta^{13}C$ $\delta^{15}N$ determinations. *Chem. Geol.* **147** (1-2), 147–159.

Cartigny, P., Harris, J.W., Taylor, A., Davies, R., Javoy, M., 2003. On the possibility of a kinetic fractionation of nitrogen stable isotopes during natural diamond growth. *Geochim. Cosmochim. Acta* **67** (8), 1571–1576.

Chinn, I.L., Gurney, J.J., Kyser, K.T., 1998. Diamonds and mineral inclusions from the NWT, Canada. In: *7th International Kimberlite Conference*, Addendum to extended abstracts, Cape Town, South Africa.

Chrenko, R., McDonald, R., Darrow, K., 1967. Infra-red spectrum of diamond coat. *Nature* **214**, 474–476.

Creaser, R.A., Grutter, H., Carlson, J., Crawford, B., 2004. Macrocrystal phlogopite Rb-Sr dates for the Ekati property kimberlites, Slave Province, Canada: evidence for multiple intrusive episodes in the Paleocene and Eocene. *Lithos* **76** (1–4), 399–414.

Dalton, J.A., Presnall, D.C., 1998. Carbonatitic melts along the solidus of model lherzolite in the system $CaO\text{-}MgO\text{-}Al_2O_3\text{-}SiO_2\text{-}CO_2$ from 3 to 7 GPa. *Contribut. Miner. Petrol.* **131** (2–3), 123–135.

Dasgupta, R., Hirschmann, M.M., Dellas, N., 2005. The effect of bulk composition on the solidus of carbonated eclogite from partial melting experiments at 3 GPa. *Contribut. Miner. Petrol.* **149** (3), 288.

Davies, R., Griffin, W.L., Pearson, N., Andrew, A., Doyle, B., O'Reilly, S., 1999. Diamonds from the deep; Pipe DO-27, Slave Craton, Canada. In: Gurney, J., Gurney, J., Pascoe, M., Richardson (Eds.), *Proceedings of the 7th International Kimberlite Conference*, vol. 1, pp. 148–155.

Davies, R.M., Griffin, W.L., O'Reilly, S.Y., Doyle, B.J., 2004. Mineral inclusions and geochemical characteristics of microdiamonds from the DO27, A154, A21, A418, DO18, DD17 and Ranch Lake kimberlites at Lac de Gras, Slave Craton, Canada. *Lithos* **77** (1–4), 39.

Falloon, P.J., Green, D.H., 1990. Solidus of carbonated fertile peridotite under fluid saturated conditions. *Geology* **18**, 195–199.

Farmer, V.C., 1974. *The Infrared Spectra of Minerals*. Mineralogical Society, London, 539 pp.

Foley, S., 1992a. Petrological characterization of the source components of potassic magmas: geochemical and experimental constraints. *Lithos* **28** (3–6), 187–204.

Foley, S., 1992b. Vein-plus-wall-rock melting mechanisms in the lithosphere and the origin of potassic alkaline magmas. *Lithos* **28** (3–6), 435–453.

Girnis, A.V., Brey, G.P., Ryabchikov, I.D., 1995. Origin of group 1a kimberlites—Fluid-saturated melting experiments at 45–55 kbar. *Earth Planet. Sci. Lett.* **134** (3–4), 283–296.

Girnis, A.V., Bulatov, V.K., Brey, G.P., 2005. Transition from kimberlite to carbonatite melt under mantle parameters: an experimental study. *Petrology* **13** (1), 1–15.

Graham, I., Burgess, J., Bryan, D., Ravenscroft, P., Thomas, E., Doyle, B., Hopkins, R., Armstrong, K., 1999. Exploration history and geology of the Diavik kimberlites, Lac de Gras, Northwest Territories, Canada. In: Gurney, J. Gurney, J., Pascoe, M., Richardson, S. (Eds.), *Proceedings of the 7th International Kimberlite Conference*, vol. 1, pp. 262–279.

Griffin, W.L., Doyle, B.J., Ryan, C.G., Pearson, N.J., O'Reilly, S.Y., Davies, R., Kivi, K., Van Achterbergh, E., Natapov, L.M., 1999. Layered mantle lithosphere in the Lac de Gras area, Slave Craton: composition, structure and origin. *J. Petrol.* **40** (5), 705–727.

Griffin, W.L., O'Reilly, S.Y., Doyle, B.J., Pearson, N.J., Coopersmith, H., Kivi, K., Malkovets, V., Pokhilenko, N., 2004. Lithosphere mapping beneath the North American plate. *Lithos* **77** (1–4), 873–922.

Gudfinnsson, G.H., Presnall, D.C., 2005. Continuous gradations among primary carbonatitic, kimberlitic, melilititic, basaltic, picritic, and komatiitic melts in equilibrium with garnet lherzolite at 3–8 GPa. *J. Petrol.* **46** (8), 1645–1659.

Gurney, J.J., Hildebrand, P.R., Carlson, J.A., Fedortchouk, Y., Dyck, D.R., 2004. The morphological characteristics of diamonds from the Ekati property, Northwest Territories, Canada. *Lithos* **77** (1–4), 21–38.

Guthrie, G.D., Veblen, D.R., Navon, O., Rossman, G.R., 1991. Submicrometer fluid inclusions in turbid-diamond coats. *Earth Planet. Sci. Lett.* **105** (1–3), 1–12.

Hammouda, T., 2003. High-pressure melting of carbonated eclogite and experimental constraints on carbon recycling and storage in the mantle. *Earth Planet. Sci. Lett.* **214** (1–2), 357–368.

Harris, J., 1992. Diamond geology. In: Field, J. (Ed.), *The Properties of Natural and Synthetic Diamonds*. Academic Press, London, pp. 345–393.

Hauri, E.H., Wang, J., Pearson, D.G., Bulanova, G.P., 2002. Microanalysis of $\delta^{13}C$, $\delta^{15}N$, and N abundances in diamonds by secondary ion mass spectrometry. *Chem. Geol.* **185** (1-2), 149–163.

Heaman, L., Kjarsgaard, B., 2000. Timing of eastern North American kimberlite magmatism: continental extension of the Great Meteor Hotspot track? *Earth Planet. Sci. Lett.* **178**, 253–268.

Hoernle, K., Tilton, G., Le Bas, M.J., Duggen, S., Garbe-Schonberg, D., 2002. Geochemistry of oceanic carbonatites compared with continental carbonatites: mantle recycling of oceanic crustal carbonate. *Contribut. Mineral. Petrol.* **142** (5), 520–542.

Ionov, D.A., Dupuy, C., Oreilly, S.Y., Kopylova, M.G., Genshaft, Y.S., 1993. Carbonated peridotite xenoliths from Spitsbergen—implications for trace-element signature of mantle carbonate metasomatism. *Earth Planet. Sci. Lett.* **119** (3), 283–297.

Izraeli, E.S., Harris, J.W., Navon, O., 2001. Brine inclusions in diamonds: a new upper mantle fluid. *Earth Planet. Sci. Lett.* **187** (3–4), 323–332.

Izraeli, E.S., Harris, J.W., Navon, O., 2003. Mineral inclusions in cloudy diamonds from Koffiefontein South-Africa. In: *8th International Kimberlite Conference*, Extended Abstracts. FLA_0113, Victoria, Canada.

Izraeli, E.S., Harris, J.W., Navon, O., 2004. Fluid and mineral inclusions in cloudy diamonds from Koffiefontein, South Africa. *Geochim. Cosmochim. Acta* **68** (11), 2561–2575.

Johnson, L., Burgess, R., Turner, G., Milledge, H., Harris, J., 2000. Noble gas and halogen geochemistry of mantle fluids: comparison of African and Canadian diamonds. *Geochim. Cosmochim. Acta* **64** (4), 717–732.

Kamenetsky, M.B., Sobolev, A.V., Kamenetsky, V.S., Maas, R., Danyushevsky, L.V., Thomas, R., Pokhilenko, N.P., Sobolev, N.V., 2004. Kimberlite melts rich in alkali chlorides and carbonates: a potent metasomatic agent in the mantle. *Geology* **32** (10), 845–848.

Kanzaki, M., 1991. Stability of hydrous magnesium silicates in the mantle transition zone. *Phys. Earth Planet. Interiors* **66** (3–4), 307–312.

Keshav, S., Corgne, A., Gudfinnsson, G.H., Bizimis, M., McDonough, W.F., Fei, Y., 2005. Kimberlite petrogenesis: insights from clinopyroxene-melt partitioning experiments at 6 GPa in the CaO-MgO-Al_2O_3-SiO_2-CO_2 system. *Geochim. Cosmochim. Acta* **69** (11), 2829–2845.

Kessel, R., Ulmer, P., Pettke, T., Schmidt, M.W., Thompson, A.B., 2005. The water-basalt system at 4 to 6 GPa: phase relations and second critical endpoint in a K-free eclogite at 700 to 1400 °C. *Earth Planet. Sci. Lett.* **237** (3–4), 873–892.

Khazan, Y., Fialko, Y., 2005. Why do kimberlites from different provinces have similar trace element patterns? *Geochem. Geophys. Geosyst.* 6, Art. No. Q10002.

Khisina, N.R., Wirth, R., 2002. Hydrous olivine $(Mg_{1-y}Fe_y^{2+})_{2-x}V_xSiO_4H_{2x}$—a new DHMS phase of variable composition observed as nanometer-sized precipitations in mantle olivine. *Phys. Chem. Miner.* **29** (2), 98–111.

Khisina, N.R., Wirth, R., Andrut, M., Ukhanov, A.V., 2001. Extrinsic and intrinsic mode of hydrogen occurrence in natural olivines: FTIR and TEM investigation. *Phys. Chem. Miner.* **28** (5), 291–301.

Klein-BenDavid, O., Logvinova, A.M., Izraeli, E., Sobolev, N.V., Navon, O., 2003. Sulfide melt inclusions in Yubileinayan (Yakutia) diamonds. In: 8*th International Kimberlite Conference*, Extended Abstracts,, FLA_0111, Victoria, Canada.

Klein-BenDavid, O., Izraeli, E.S., Hauri, E., Navon, O., 2004. Mantle fluid evolution—a tale of one diamond. *Lithos* **77** (1–4), 243–253.

Klein-BenDavid, O., Wirth, R., Navon, O., 2006. TEM imaging and analysis of microinclusions in diamonds: a close look at diamond-growing fluids. *Am. Mineral.* **91**, 353–365.

Komabayashi, T., Omori, S., Maruyama, S., 2004. Petrogenetic grid in the system MgO-SiO_2-H_2O up to 30 GPa, 1600 °C: applications to hydrous peridotite subducting into the Earth's deep interior. *J. Geophys. Res. Solid Earth* **109** (B3).

Lang, A.R., Walmsley, J.C., 1983. Apatite inclusions in natural diamond coat. *Phys. Chem. Miner.* **9** (1), 6–8.

Le Roex, A.P., Bell, D.R., Davis, P., 2003. Petrogenesis of group I kimberlites from Kimberley, South Africa: evidence from bulk-rock geochemistry. *J. Petrol.* **44** (12), 2261–2286.

Liu, F.S., Hong, S.M., Jing, F.Q., 2002. Solubility of carbon in high-pressure and high-temperature water. *J. Phys.-Condensed Matter* **14** (44), 11431–11435.

Logvinova, A.M., Klein-BenDavid, O., Izraeli, E.S., Navon, O., Sobolev, N.V., 2003. Micro-inclusions in fibrous diamonds from Yubileinaya kimberlite pipe (Yakutia). In: *8th International Kimberlite Conference*, Extended Abstracts, FLA_0025, Victoria, Canada.

Maas, R., Kamenetsky, M.B., Sobolev, A.V., Kamenetsky, V.S., Sobolev, N.V., 2005. Sr, Nd, and Pb isotope evidence for a mantle origin of alkali chlorides and carbonates in the Udachnaya kimberlite, Siberia. *Geology* **33** (7), 549–552.

Mernagh, T.P., Liu, L.G., 1998. Raman and infrared spectra of phase E, a plausible hydrous phase in the mantle. *Canad. Mineral.* **36**, 1217–1223.

Meyer, H.O.A., 1987. Inclusions in diamond. In: Nixon, P.H. (Ed.), *Mantle Xenoliths*. John Wiley, Chichester, UK, pp. 501–522.

Milledge, H., Mendelssohn, M., Woods, P., Seal, M., Pillinger, C., Mattey, D., Carr, L., Wright, I., 1984. Isotopic variations in diamond in relation to cathodoluminescence. *Acta Crystallogr., Sect. A: Foundations Crystallogr.* **40**, 255.

Mitchell, R.H., 1986. The nature of kimberlites. In: Smith, C. (Ed.), *Fourth International Kimberlite Conference*. Geological Society of Australia, Perth.

Mitchell, R.H., Bergman, S.C., 1991. *Petrology of Lamproites*. Plenum press, New York, 447 pp..

Mitchell, R.H., Edgar, A.D., 2002. Melting experiments on SiO_2-rich lamproites to 6.4 GPa and their bearing on the sources of lamproite magmas. *Mineral. Petrol.* **74** (2–4), 115–128.

Navon, O., 1991. High internal-pressures in diamond fluid inclusions determined by infrared-absorption. *Nature* **353** (6346), 746–748.

Navon, O., 1999. Formation of diamonds in the Earth's mantle. In: Gurney, J., Richardson, S., Bell, D. (Eds.), *Proceedings of the 7th International Kimberlite Conference*. Red Roof Designs, Cape Town, South Africa, pp. 584–604.

Navon, O., Stolper, E., 1987. Geochemical consequences of melt percolation—the upper mantle as a chromatographic column. *J. Geol.* **95** (3), 285–307.

Navon, O., Hutcheon, I.D., Rossman, G.R., Wasserburg, G.J., 1988. Mantle-derived fluids in diamond micro-inclusions. *Nature* **335** (6193), 784–789.

Navon, O., Izraeli, E.S., Klein-BenDavid, O., 2003. Fluid inclusions in diamonds—the Carbonatitic connection. In: *8th International Kimberlite Conference*, Extended abstracts, FLA_0107, Victoria, Canada.

Nelson, D.R., Chivas, A.R., Chappell, B.W., McCulloch, M.T., 1988. Geochemical and isotopic systematics in carbonatites and implications for the evolution of ocean-island sources. *Geochim. Cosmochim. Acta* **52** (1), 1–17.

Pal'yanov, Y.N., Sokol, A.G., Borzdov, Y.M., Khokhryakov, A.F., Sobolev, N.V., 1999. Diamond formation from mantle carbonate fluids. *Nature* **400** (6743), 417–418.

Pal'yanov, Y.N., Sokol, A.G., Sobolev, N.V., 2005. Experimental modeling of mantle diamond-forming processes. *Russ. Geol. Geophys.* **46** (12), 1271–1284.

Perchuk, L.L., Safonov, O.G., Yapaskurt, V.O., Barton, J.M., 2002. Crystal-melt equilibria involving potassium-bearing clinopyroxene as indicator of mantle-derived ultrahigh-potassic liquids: an analytical review. *Lithos* **60** (3–4), 89–111.

Price, S.E., Russell, J.K., Kopylova, M.G., 2000. Primitive magma from the Jericho Pipe, NWT, Canada: constraints on primary kimberlite melt chemistry. *J. Petrol.* **41** (6), 789–808.

Rao, N.V.C., Gibson, S.A., Pyle, D.M., Dickin, A.P., 2004. Petrogenesis of Proterozoic lamproites and kimberlites from the Cuddapah Basin and Dharwar Craton, southern India. *J. Petrol.* **45** (5), 907–948.

Rege, S., Jackson, S., Griffin, W.L., Davies, R.M., Pearson, N.J., O'Reilly, S.Y., 2005. Quantitative trace-element analysis of diamond by laser ablation inductively coupled plasma mass spectrometry. *J. Anal. Atomic Spectr.* **20** (7), 601–611.

Roedder, E., 1992. Fluid Inclusion evidence for immiscibility in magmatic differentiation. *Geochim. Cosmochim. Acta* **56** (1), 5–20.

Salvioli-Mariani, E., Toscani, L., Bersani, D., 2004. Magmatic evolution of the Gaussberg lamproite (Antarctica): volatile content and glass composition. *Mineral. Mag.* **68** (1), 83–100.

Scambelluri, M., Philippot, P., 2001. Deep fluids in subduction zones. *Lithos* **55** (1–4), 213–227.

Schmidt, M.W., Vielzeuf, D., Auzanneau, E., 2004. Melting and dissolution of subducting crust at high pressures: the key role of white mica. *Earth Planetary Sci. Lett.* **228** (1–2), 65–84.

Schrauder, M., Navon, O., 1994. Hydrous and carbonatitic mantle fluids in fibrous diamonds from Jwaneng, Botswana. *Geochim. Cosmochim. Acta* **58** (2), 761–771.

Schrauder, M., Koeberl, C., Navon, O., 1996. Trace element analyses of fluid-bearing diamonds from Jwaneng, Botswana. *Geochim. Cosmochim. Acta* **60** (23), 4711–4724.

Shatsky, A.F., Borzdov, Y.M., Sokol, A.G., Pal'yanov, Y.N., 2002. Phase formation and diamond crystallization in carbon-bearing ultrapotassic carbonate-silicate systems. *Geol. Geofiz.* **43** (10), 940–950.

Shiryaev, A.A., Izraeli, E.S., Hauri, E.H., Zakharchenko, O.D., Navon, O., 2005a. Chemical, optical and isotopic investigation of fibrous diamonds from Brazil. *Russ. Geol. Geophys.* **46** (12), 1185–1201.

Shiryaev, A.A., Spivak, A.V., Litvin, Yu.A., Urusov, V.S., 2005b. Formation of nitrogen A-defects in diamond during growth in carbonate–carbon solutions-melts: experiments at 5.5–8.5 GPa. *Doklady Earth Sci.* **403A** (6), 908–911.

Smith, C.B., Gurney, J.J., Harris, J.W., Otter, M.L., Kirkley, M.B., Jagoutz, E., 1991. Neodymium and strontium isotope systematics of eclogite and websterite paragenesis inclusions from single diamonds,

Finsch and Kimberley pool, Rsa. *Geochim. Cosmochim. Acta* **55** (9), 2579–2590.

Sobolev, N., Kaminsky, F., Griffin, W., Yefimova, E., Win, T., Ryan, C., Botkunov, A., 1997. Mineral inclusions in diamonds from the Sputnik kimberlite pipe, Yakutia. *Lithos* **39** (3-4), 135–157.

Sobolev, N.V., Sobolev, V.N., Snyder, G.A., Yefimova, E.S., Taylor, L.A., 1999. Significance of eclogitic and related parageneses of natural diamonds. *Int. Geol. Rev.* **41** (2), 129–140.

Spivak, A.V., Litvin, Y.A., 2004. Diamond syntheses in multicomponent carbonate-carbon melts of natural chemistry: elementary processes and properties. *Diamond Related Mater.* **13** (3), 482–487.

Sunagawa, I., 1984. Morphology of natural and synthetic diamond crystals. In: Sunagawa, I. (Ed.), *Materials Science of the Earth's interior*. Terra Scientific, Tokyo, pp. 303–330.

Sweeney, R.J., 1994. Carbonatite melt compositions in the earth's mantle. *Earth Planet. Sci. Lett.* **128** (3-4), 259–270.

Tal'nikova, S.B., 1995. Inclusions in natural diamonds of different habits. In: *6th International Kimberlite Conference*, Extended Abstracts, 603–605. Novosibirsk, Russia.

Tappert, R., Stachel, T., Harris, J.W., Shimizu, N., Brey, G.P., 2005. Mineral inclusions in diamonds from the Panda kimberlite, Slave Province, Canada. *Eur. J. Mineral.* **17** (3), 423–440.

Taylor, L.A., Anand, M., 2004. Diamonds: time capsules from the Siberian Mantle. *Chemie der Erde-Geochem.* **64** (1), 1–74.

Taylor, L.A., Keller, R.A., Snyder, G.A., Wang, W.Y., Carlson, W.D., Hauri, E.H., McCandless, T., Kim, K.R., Sobolev, N.V., Bezborodov, S.M., 2000. Diamonds and their mineral inclusions, and what they tell us: a detailed "pull-apart" of a diamondiferous eclogite. *Int. Geol. Rev.* **42** (11), 959–983.

Thibault, Y., Edgar, A.D., Lloyd, F.E., 1992. Experimental investigation of melts from a carbonated phlogopite lherzolite—implications for metasomatism in the continental lithospheric mantle. *Am. Mineral.* **77** (7-8), 784–794.

Tomilenko, A.A., Chepurov, A.I., Pal'yanov, Y.N., Pokhilenko, L.N., Shebanin, A.P., 1997. Volatile components in the upper mantle (from data on fluid inclusions). *Geol. Geofiz.* **38** (1), 276–285.

Turner, G., Burgess, R., Bannon, M., 1990. Volatile-rich mantle fluids inferred from Inclusions in diamond and mantle xenoliths. *Nature* **344** (6267), 653–655.

van Achterbergh, E., Griffin, W.L., Ryan, C.G., O'Reilly, S.Y., Pearson, N.J., Kivi, K., Doyle, B.J., 2002. Subduction signature for quenched carbonatites from the deep lithosphere. *Geology* **30** (8), 743–746.

Wada, N., Matsuda, J.I., 1998. A noble gas study of cubic diamonds from Zaire: constraints on their mantle source. *Geochim. Cosmochim. Acta* **62** (13), 2335–2345.

Wallace, M.E., Green, D.H., 1988. An experimental-determination of primary carbonatite magma composition. *Nature* **335** (6188), 343–346.

Walmsley, J.C., Lang, A.R., 1992a. On submicrometer inclusions in diamond coat—crystallography and composition of ankerites and related rhombohedral carbonates. *Mineral. Mag.* **56** (385), 533–543.

Walmsley, J.C., Lang, A.R., 1992b. Oriented biotite Inclusions in diamond coat. *Mineral. Mag.* **56** (382), 108–111.

Wannamaker, P.E., Hulen, J.B., Heizler, M.T., 2000. Early Miocene lamproite from the Colorado Plateau tectonic province, Southeastern Utah, USA. *J. Volcanol. Geothermal Res.* **96** (3–4), 175–190.

Woods, G.S., Purser, G.C., Mtimkulu, A.S.S., Collins, A.T., 1990. The nitrogen-content of Type Ia natural diamonds. *J. Phys. Chem. Solids* **51** (10), 1191–1197.

Woolley, A.R., Kempe, D.R.C., 1989. Carbonatites: nomenclature, average chemical compositions, and element distribution. In: Bell, K. (Ed.), *Carbonatites: Genesis and Evolution*. Unwin Hyman, pp. 1–14.

Wyllie, P., 1989. The genesis of kimberlites and some low-SiO_2, high-alkali magmas. In: Ross, J., Jaques, A., Ferguson, J., Green, D., O'Reilly, S., Danchin, R., Janse, A. (Eds.), *Kimberlites and Related Rocks*, vol. 14, pp. 603–615.

Wyllie, P.J., Huang, W.L., 1975. Influence of mantle CO_2 in the generation of carbonatites and kimberlites. *Nature* **257**, 297–299.

Wyllie, P.J., Ryabchikov, I.D., 2000. Volatile components, magmas, and critical fluids in upwelling mantle. *J. Petrol.* **41** (7), 1195–1206.

Yaxley, G.M., 1999. Phase relations in carbonated eclogite under upper mantle PT conditions—implications for carbonatite petrogenesis. In: Gurney, J., Richardson, S., B ell, D. (Eds.), *Proceedings of the 7th International Kimberlite Conference*. Red Roof Designs, Cape Town, South Africa, pp. 923–947.

Yaxley, G.M., Brey, G.P., 2004. Phase relations of carbonate-bearing eclogite assemblages from 2.5 to 5.5 GPa: implications for petrogenesis of carbonatites. *Contribut. Mineral. Petrol.* **146** (5), 606–619.

Yaxley, G.M., Green, D.H., 1994. Experimental demonstration of refractory carbonate-bearing eclogite and siliceous melt in the subduction regime. *Earth Planet. Sci. Lett.* **128** (3–4), 313–325.

Yaxley, G.M., Green, D.H., 1998. Reactions between eclogite and peridotite: mantle refertilisation by subduction of oceanic crust. *Schweizerische Mineral. Petrogr. Mitteilungen* **78** (2), 243–255.

Yaxley, G.M., Crawford, A.J., Green, D.H., 1991. Evidence for carbonatite metasomatism in spinel peridotite xenoliths from Western Victoria, Australia. *Earth Planet. Sci. Let.* **107** (2), 305–317.

Zedgenizov, D.A., Kagi, H., Shatsky, V.S., Sobolev, N.V., 2004. Carbonatitic melts in cuboid diamonds from Udachnaya kimberlite pipe (Yakutia): evidence from vibrational spectroscopy. *Mineral. Mag.* **68** (1), 61–73.